DOI: 10.1534/genetics.106.057166

Localization of Müllerian Mimicry Genes on a Dense Linkage Map of *Heliconius erato*

Durrell D. Kapan,*[,1] Nicola S. Flanagan,*[,2] Alex Tobler,*[,3] Riccardo Papa,* Robert D. Reed,[†] Jenny Acevedo Gonzalez,* Manuel Ramirez Restrepo,* Lournet Martinez,* Karla Maldonado,* Clare Ritschoff,[‡] David G. Heckel[§] and W. Owen McMillan*

*Department of Biology, University of Puerto Rico, San Juan, PR 00931, [†]Department of Biology, Duke University, Durham, NC 27708-0338, [‡]Department of Biology, Cornell University, Ithaca, New York 14853 and [§]Max Planck Institute of Chemical Ecology, D-07745 Jena, Germany

Manuscript received September 9, 2005
Accepted for publication February 15, 2006

ABSTRACT

We report a dense genetic linkage map of *Heliconius erato*, a neotropical butterfly that has undergone a remarkable adaptive radiation in warningly colored mimetic wing patterns. Our study exploited natural variation segregating in a cross between *H. erato etylus* and *H. himera* to localize wing color pattern loci on a dense linkage map containing amplified fragment length polymorphisms (AFLP), microsatellites, and single-copy nuclear loci. We unambiguously identified all 20 autosomal linkage groups and the sex chromosome (*Z*). The map spanned a total of 1430 Haldane cM and linkage groups varied in size from 26.3 to 97.8 cM. The average distance between markers was 5.1 cM. Within this framework, we localized two major color pattern loci to narrow regions of the genome. The first gene, *D*, responsible for red/orange elements, had a most likely placement in a 6.7-cM region flanked by two AFLP markers on the end of a large 87.5-cM linkage group. The second locus, *Sd*, affects the melanic pattern on the forewing and was found within a 6.3-cM interval between flanking AFLP loci. This study complements recent linkage analysis of *H. erato*'s comimic, *H. melpomene*, and forms the basis for marker-assisted physical mapping and for studies into the comparative genetic architecture of wing-pattern mimicry in Heliconius.

RECENT advances in molecular biology allow researchers to directly investigate the genetic basis of adaptive variation in natural populations of widely divergent organisms, ranging from Mimulus and crickets to sticklebacks and pocket mice (Bradshaw *et al.* 1998; Peichel *et al.* 2001; Parsons and Shaw 2002; Albertson *et al.* 2003; Hoekstra *et al.* 2004; Nachman *et al.* 2004; Colosimo *et al.* 2005). This research has allowed novel insights into the mechanisms governing morphological diversification by coupling traditional studies of ecological genetics and natural selection with modern genomic approaches.

In this article, we localize two major color pattern loci underlying adaptive variation in the wing patterns of *Heliconius erato* to narrow regions of a high-resolution genetic map. This work replaces an initial linkage map of *H. erato* (Tobler *et al.* 2005), and complements a recently published high-resolution linkage map of its comimic *H. melpomene* (Jiggins *et al.* 2005). The nearly identical wing color patterns of *H. erato* and *H. melpomene* not only are adaptations that warn potential predators of each species' unpalatability (Chai 1986; Langham 2005) and a textbook example of cooperative or Müllerian mimicry (Müller 1879; Nijhout 1991), but also play an important role in speciation (McMillan *et al.* 1997; Jiggins *et al.* 2001). Although these species are from divergent clades within the genus and do not hybridize, they share nearly identical color pattern phenotypes where they co-occur and have undergone a parallel adaptive radiation into nearly 30 different geographic races (Brown *et al.* 1974; Turner 1974, 1983; Sheppard *et al.*, 1985; Brower 1994, 1996; Turner and Mallet 1997; Beltrán *et al.* 2002).

Within each species interracial crossing experiments have described up to 20 different loci responsible for this wing color pattern diversification (Sheppard *et al.* 1985; Mallet 1989; Nijhout *et al.* 1990, 1991; Jiggins and McMillan 1997; Gilbert 2003; Naisbit *et al.* 2003). However, one of the most striking aspects of both radiations is that the majority of phenotypic change is driven by a small number of loci, or groups of very tightly linked loci, of large effect (Sheppard *et al.* 1985; Mallet 1989; Nijhout *et al.* 1990; Nijhout 1991; Jiggins and McMillan 1997; Gilbert 2003; Naisbit *et al.* 2003). These major genes cause discrete phenotypic shifts across large areas of the wing surface by changing the

[1]*Corresponding author:* Center for Conservation and Research Training, Pacific Biosciences Research Center, 3050 Maile Way, Gilmore 406, University of Hawaii, Manoa, Honolulu, HI 96822.
E-mail: durrell@hawaii.edu

[2]*Present address:* School of Botany and Zoology, The Australian National University, Canberra, ACT 0200 Australia.

[3]*Present address:* Department of Biology, Duke University, Durham, North Carolina 27708-0338

position, size, and shape of red/orange and melanic patches on both the dorsal and ventral surfaces of the fore- and hindwings (Sheppard *et al.* 1985; Nijhout 1991). In both radiations, the genes underlying different pattern elements have a predictable epistatic effect depending on scale and pigment type (Gilbert *et al.* 1988; Gilbert 2003). These facts make it relatively easy to follow the segregation of specific alleles at a locus in genetic backgrounds chosen to minimize epistasis (Tobler *et al.* 2005).

Characterization of genomic regions directly responsible for adaptive differences in wing color patterns in both these species will allow us to answer questions about the proximate and ultimate origins of this fascinating variation. As an important step toward this goal, we report the localization of two major *H. erato* color pattern switch genes within a high-resolution linkage map: the "Dennis" (or *D*) locus responsible for red and orange pattern elements and the "shortened" (*Sd*) locus that affects forewing melanin patterns (Sheppard *et al.* 1985). In contrast to our preliminary study (Tobler *et al.* 2005), which utilized fewer markers and individuals in a backcross design, we trace inheritance patterns of numerous molecular markers and wing phenotypes in a large outbred F_2 cross (*i.e.*, with two pairs of unrelated outbred grandparents). For this study, we crossed an orange and yellow race from southeast Ecuador *H. erato etylus* with *H. himera*, a closely related sister species from south Ecuador that displays yellow and bright red (see Figure 1; Tobler *et al.* 2005). In *H. erato* races the *D* locus controls the presence of the orange and red elements, including (1) the orange patch at the base of the forewing in *H. erato etylus* known as "Dennis" [after an individual *H. melpomene* with the mimetic phenotype named "Dennis the Menace" (Beebe 1955); see also Sheppard *et al.* 1985, p. 457; J. Mallet, personal communication], (2) the orange rays present on the hindwing of many Amazonian races (Sheppard *et al.* 1985; Mallet 1989), (3) the yellow forewing band of several Amazonian races (Sheppard *et al.* 1985), and (4) the red hindwing bar in *H. himera* (Figure 1; Jiggins and McMillan 1997; Tobler *et al.* 2005). Genetic control of the first three pattern elements was initially hypothesized to be controlled by three separate, albeit tightly linked loci (*D*, *R*, and *y*, Sheppard *et al.* 1985), but recombinant phenotypes are virtually unknown from thousands of field-caught individuals along hybrid zones (Sheppard *et al.* 1985; Mallet 1989) and virtually absent from crossing experiments, suggesting that the phenotypic variation may be explained by allelic variation at a single locus or possibly three very tightly linked loci (see Sheppard *et al.* 1985; Mallet 1989; Jiggins and McMillan 1997). In this article, in accordance with nomenclature established by Jiggins and McMillan (1997), we utilize D^{et} to describe the *H. erato etylus* allele (with the "*DRy*" pattern) of the *D* locus and demonstrate through Mendelian cosegregation and mapping that the presence or absence of the red hindwing bar in *H. himera* is in fact due to *D* locus variation (D^{hi}) as initially hypothesized by Jiggins and McMillan (1997) and subsequently mapped to one end of chromosome HEC 3 (Tobler *et al.* 2005).

The *Sd* locus is one of several genes affecting melanization in the forewing (Sheppard *et al.* 1985) and was originally described from a single cross between a hybrid east Ecuador *H. erato* (*lativitta* × *notabilis*) and an east Brazilian race of *H. erato* where *Sd* accounted for shortening of the forewing yellow band (Sheppard *et al.*, 1985). In our cross, however, two complementary *Sd* patterns were found: In *H. erato etylus*, individuals had a yellow patch present toward the distal tip of the forewing and absent more proximally (genotype Sd^{et} Sd^{et}, Figure 1a, individuals PR222 and PR217), and, conversely, *H. himera* has a proximal yellow patch (genotype Sd^{hi} Sd^{hi}, Figure 1a, individuals PR246 and PR181).

To construct a linkage map we mapped molecular markers including amplified fragment length polymorphisms (AFLP), microsatellites, and single copy nuclear loci (SCNL) in F_2 offspring utilizing a three-step method based on Jiggins *et al.* (2005) and outlined in supplemental Figure S1 (http://www.genetics.org/supplemental/). This method takes advantage of natural variation within our source populations and achiasmatic oogenesis, which leads to a complete absence of crossing over in female Lepidoptera (Suomalainen *et al.* 1971, 1973; Turner and Smiley 1975) to generate a single high-resolution genetic map for the cross. This map provides the basis for localizing color pattern loci in specific genomic regions, generating an integrated reference map of all the major color pattern genes responsible for the *H. erato* diversification, and is an essential step toward our goal of understanding the genetic architecture of convergent evolution between *H. erato* and its comimic, *H. melpomene*.

MATERIALS AND METHODS

Crossing design: To identify major wing pattern loci in the Amazonian rayed race under study, we collected individuals of *H. erato etylus* from the Zamora River (3°55′ S, 78°50′ W) and individuals of *H. himera* from the town of Vilcabamba (4°16′ S, 79°13′ W), both in Loja Province in southern Ecuador, with permits from the Ecuadorian government (Tobler *et al.* 2005). Outbred stocks of both *H. erato etylus* and *H. himera* were established in our insectaries at the University of Puerto Rico. From these stocks we created an outbred F_2 cross, designated ETF2-2, by mating two unrelated F_1 hybrids derived from unrelated *H. erato etylus* female and *H. himera* male grandparents (Figure 1, A and B). Butterflies were cared for as outlined in McMillan *et al.* (1997). The 88 F_2 offspring in the brood were raised until eclosion and killed by briefly exposing them to −80°. The bodies were frozen at −80° until needed and the wings were digitally photographed and preserved in glassine envelopes for later analysis.

AFLPs: Genomic DNA was extracted as outlined in Tobler *et al.* (2005). AFLP analysis followed protocols described by Vos *et al.* (1995) with modifications for fluorescent-labeled AFLP reactions run on an ABI PRISM 377 DNA sequencer

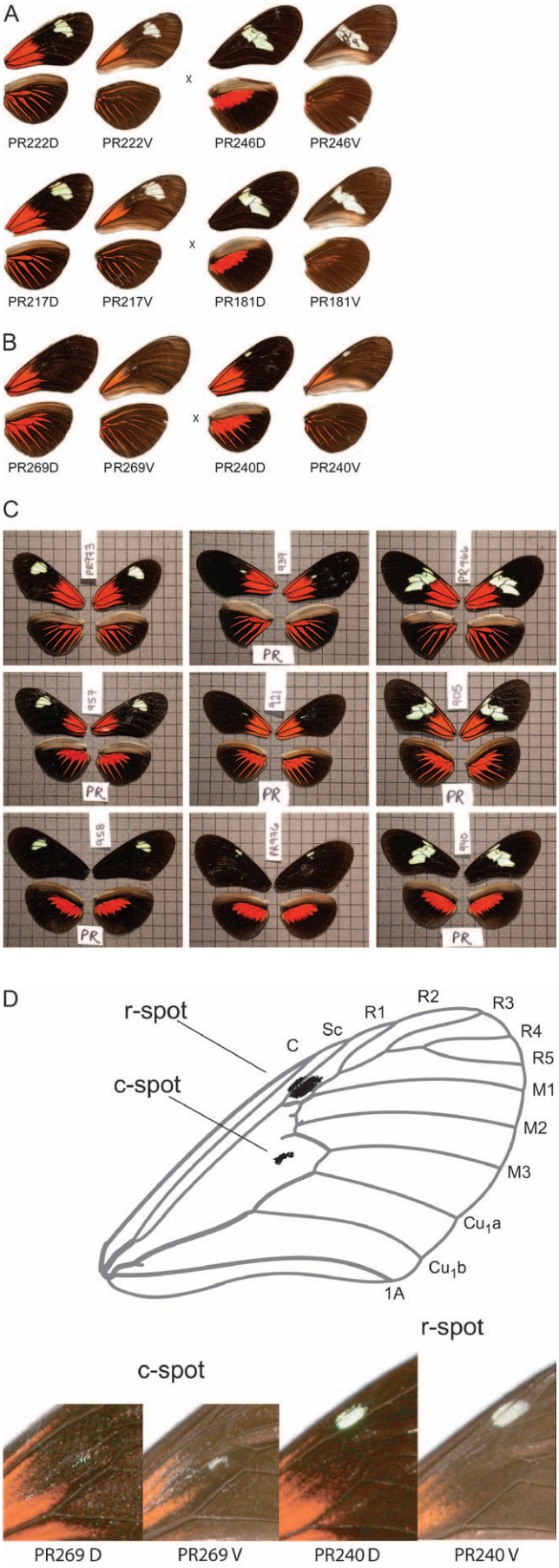

(Applied Biosystems) as outlined by Tobler *et al.* (2005). We surveyed 20 *Eco*RI/*Mse*I primer combinations for fragments between ~100 and 500 bp in length (Table 1, supplemental Appendix at http://www.genetics.org/supplemental/). Size-corrected data for all individuals and control lanes were combined into a metagel for each primer combination using a modified version of Genographer (Benham *et al.* 1999), an open source java program for AFLP analysis (http://hordeum.oscs.montana.edu/genographer/). The modified version (2.1 beta) is currently available for download (http://zephyr.hp*cf.*upr.edu/~mcmi-lab/). AFLP bands were scored as present if a distinct band appeared on the metagel (either in normalized or in unnormalized view within Genographer) and accompanying peaked fluorescent signal was seen using the thumbnail view in Genographer and absent otherwise (weakly amplifying lanes with shallow, indistinct peaks were scored as missing data). All AFLP bands were scored as dominant alleles (*i.e.*, no attempt was made to infer heterozygosity from reduced band intensity). Fluorescent bands were named according to primer combination and band size in base pairs (see supplemental Appendix, http://www.genetics.org/supplemental/). Overall, ~70,760 (610 AFLP loci × 116 lanes = 16 grandparental replicates, 12 parental replicates, and 88 offspring) binary genotypes were individually examined by one or more investigators before export from Genographer as a matrix of zeroes and ones.

Codominant anchor loci: We also scored microsatellite and SCNL to anchor our maps relative to other mapping work in Heliconius. We surveyed variation at 19 microsatellites (Table 2) and 21 SCNL (Table 3). Microsatellites were amplified and scored as described in Flanagan *et al.* (2002) and Tobler *et al.* (2005) and Table 2. SCNL for a variety of candidate and housekeeping genes were utilized and segregating genotypes were determined using allelic size variation or by variation at single nucleotide positions (Table 3) (Jiggins *et al.* 2005; Tobler *et al.* 2005). Single nucleotide polymorphisms (SNPs) were scored by restriction fragment length polymorphism (Jiggins *et al.* 2005; Tobler *et al.* 2005) generated by restriction enzymes (under the conditions recommended by the

Figure 1.—Cross design and cosegregating wing phenotypes all shown with right dorsal (left) and left ventral (right) fore- and hindwings. (A) The outbred F_2 cross shown with maternal grandmother PR222 (*H. erato etylus*) × maternal grandfather PR246 (*H. himera*); paternal grandmother PR217 (*H. erato etylus*) × paternal grandfather PR181 (*H. himera*). PR246 displays a cage code used to identify individuals on the ventral side. (B) The F_1 female PR269 (daughter of PR222 and PR246) was mated to F_1 male PR240 (the son of PR217 and PR181). (C) Codominant phenotypic effects of two major loci segregating in F_2 offspring can be seen with columns representing the three *Sd* genotypes: $Sd^{et}Sd^{et}$, $Sd^{et}Sd^{hi}$, and $Sd^{hi}Sd^{hi}$, respectively. The rows represent the three *D* genotypes: $D^{et}D^{et}$, $D^{et}D^{hi}$, and $D^{hi}D^{hi}$. Thus the top left butterfly and the bottom right butterfly resemble their respective grandparents, *H. erato etylus* and *H. himera*, respectively. (D) Small spot phenotypes. PR269 dorsal and ventral showing inheritance of the yellow discal cell spot (c-spot) from female *H. erato etylus* PR222, and PR240 dorsal and ventral showing the yellow R2-R1 spot (r-spot) inherited from female PR217. Both *H. erato etylus*-derived spot genotypes are visible only when present in heterozygous form with the *H. himera Sd* allele; see, for instance, the middle individual PR921 in C showing the c-spot phenotype and the bottom row individual PR976 in C showing the r-spot (wing vein drawing modified from Emsley 1963).

TABLE 1

Summary of AFLP primer combinations and total number of polymorphic bands utilized in our analysis

		*Mse*I extension								
*Eco*RI extension	Data	CAA	CAC	CAG	CCA	CCT	CTA	CTG	CTT	Total
CA	*FI*	14	10	9	10			2		45
	BI	18	7	13	14			8		60
	MI	12	9	9	9			2		41
CC	*FI*	10		7			0		10	27
	BI	2		4			0		7	13
	MI	8		7			0		6	21
CG	*FI*	15	13	10					7	45
	BI	12	6	10					8	36
	MI	18	14	9					6	47
CT	*FI*	3	22	10		10	13	8	8	74
	BI	9	30	11		7	10	3	3	73
	MI	4	23	16		11	9	10	8	81
Total	*FI*	42	45	36	10	10	13	10	25	191
	BI	41	43	38	14	7	10	11	18	182
	MI	42	46	41	9	11	9	12	20	190
	All	125	134	115	33	28	32	33	63	563

These totals do not include bands generated by the second metabulk scan for tightly linked markers generated by primer combinations *Eco*-CC *Mse*I-CTA/CTT, *Eco*-CT *Mse*I-CTA/CTT, and new combinations *Eco*-CC/*Mse*ICTC, *Eco*-CC/*Mse*I-CAC run utilizing *Licor* methodology (Tobler *et al.* 2005). An additional eight male informative bands were scored. For details see map and supplemental Appendix (http://www.genetics.org/supplemental/) for bands *CC-CTA_Sd_120-145*, *CC-CTA*mbA*, *CT-CTT*mbA*, *CC- CTT_Sd_255*, *CT-CTA_DRY_2524*, *CT-CTT_DRY_>204*, *CC-CTC_Sd_145-175*, and *CC-CAC-491*. Blanks indicate the primer combination was not assayed.

vendors) or using the MegaBACE SNuPe Genotyping Kit (Amersham Biosciences). In the SNuPe technique, PCR primers are used to amplify a fragment containing a previously detected SNP, followed by a single-base extension from an unlabeled primer adjacent to the SNP site. Each dNTP in the extension mix is labeled with a different dye allowing detection of heterozygotes and homozygotes by electrophoresis on the MegaBACE system. A total of 5 μl of the PCR reaction was incubated with 6 units of exonuclease and 0.45 units of shrimp alkaline phosphatase in a final volume of 8.0 μl. The mix was heated to 37° for 30 min then denatured at 85° for 10 min. Approximately 6 ng of PCR product was combined with 2 pmol of the SNP primer and 0.5 μl (one-eighth of that recommended by the vendor) of the SNuPe premix reagent in a final volume of 10 μl. The reaction was cycled 25 times through the following temperature profile: 96° for 10 sec, 50° for 5 sec, and 60° for 10 sec. SNuPe reactions were cleaned using AutoSeq96 plates (Amersham Biosciences). After washing the columns twice with 100 μl of double-distilled water, samples were added to the top of the Sephadex and centrifuged for 5 min at 910 × *g*. Five microliters of the cleaned SNuPe reaction were added to a skirted 96-well plate and combined with 5 μl of a master mix containing 498.75 μl of MegaBACE loading solution and 1.25 μl of MegaBACE SNuPe multiple injection marker (Amersham Biosciences). Samples were injected into the MegaBACE using the protocols outlined in the user manual.

Linkage analysis and map construction: Linkage analysis followed methods for Lepidoptera published by Shi *et al.* (1995), Yasukochi (1998), Tobler *et al.* (2005), and Jiggins *et al.* (2005). By separately treating the three different genotypes corresponding to the dominant AFLP bands segregating in this cross, a single map was constructed in a three-step process (Jiggins *et al.* 2005; see Figure S1 at http://www.genetics.org/supplemental/). Bands from female-informative (FI) AFLP markers are present in the F_1 female, absent from the F_1 male, and segregate 1:1 (*e.g.*, band positive *vs.* band absent) in the F_2 progeny. Bands from male-informative (MI) markers are present in the F_1 male, absent from the F_1 female, and also segregate 1:1 in the F_2 progeny. Bands present in both F_1 male and female parents (BI markers) segregate in a 3:1 ratio in the F_2 progeny. The FI and MI marker types are rare or absent in F_2 crosses formed by crossing highly inbred strains, but are abundant in outbred F_2 crosses such as ours, where the four grandparents are polymorphic.

In step one, FI markers are used to identify linkage groups segregating in the female F_1 gametes. Because of achiasmatic oogenesis in Lepidoptera, FI markers on the same chromosome are inherited as a unit and this association is not broken up by crossing over (Jiggins *et al.* 2005). We identified 21 linkage groups by grouping these FI markers at LOD 8.0 using JoinMap 3.0 (Van Ooijen and Voorrips 2001) applied to a backcross design. By observing which FI alleles originated from *H. himera* and which from *H. erato etylus*, we predicted the species origin of the maternally derived homolog of every chromosome in each of the F_2 offspring [known as the chromosome print, Yasukochi (1998)] using PERL script "CHROMPRINT" (http://zephyr.hpcf.upr.edu/~mcmi-lab/), which compared the genotype of each offspring and linkage phase of each FI locus within a linkage group. Each chromosome print was hand verified and numbered (LG-#) to uniquely associate FI linkage groups with BI and MI markers (see below and supplemental Appendix at http://www.genetics.org/supplemental/).

TABLE 2

Summary of microsatellite anchor loci used in this study

Marker name	Primer name	Primer sequence	Reaction conditions	No. of alleles	Mapping group	Notes	Source (GenBank no.)
Hel-03	GA-7F	5′-CCAATTATGTCACATGGATCTGTT-3′	54°; 3.0 mM	2	[a]	[b]	Flanagan *et al.* (2002)
	GA-7R	5′-CTCTGTCGTCCTCTGCAGTC-3′	$MgCl_2$				
Hel-04	GA-8F	5′-GGAACGGAGTGCCCTAAAAC-3′	55°; 3.0 mM	3	HEE 7		Flanagan *et al.* (2002)
	GA-8R	5′-CGTTGCCGCTTATACTTTCC-3′	$MgCl_2$				
Hel-05	GA-11F	5′-TGCTGTCCATACCCAACTCA-3′	55°; 3.0 mM	NA	[a]	[c]	Flanagan *et al.* (2002)
	GA-11R	5′-CGAACTCACAACCATCAGTCA-3′	$MgCl_2$				
Hel-06	GA-16F	5′-TAGCCTTCACTTTGAACCCG-3′	55°; 3.0 mM	2	HEC Z	Sex-linked	Flanagan *et al.* (2002)
	GA-16R	5′-CCCACTCGAAGCAATGAAAT-3′	$MgCl_2$				
Hel-07	GA-19F	5′-GCGGGGACAACTACATAAGC-3′	55°; 3.0 mM	2	HEE 13	Alternative allele of *Hel-01* (B6), sex-linked in Tobler *et al.* (2005)	Flanagan *et al.* (2002)
	GA-19R	5′-CCCGAACCACTAAAGTCGAA-3′	$MgCl_2$				
Hel-01	B6F	5′-AGGGCGTCGTTAGTTTGTGT-3′	54°; 3.0 mM	2	HEE 13	Alternative allele of *Hel-07* (GA19), sex-linked in Tobler *et al.* (2005)	Flanagan *et al.* (2002)
	B6R	5′-TCGTAGATATCCATTACTCTGGTCTG-3′	$MgCl_2$				
Hel-10	CA-9F	5′-TCTCACTTTCCCACACAGCA-3′	55°; 3.0 mM	2	HEC 10		Flanagan *et al.* (2002)
	CA-9R	5′-TGTGAAGAGACACATGGGGA-3′	$MgCl_2$				
Hel-11	CA-10F	5′-TTTCTTTTGAGTCCCGATGG-3′	55°; 3.0 mM	3	HEC 12	Alternative allele of *Hel-08* (A2)	Flanagan *et al.* (2002)
	CA-10R	5′-ATCTCAGAACTGGTCGGCAG-3′	$MgCl_2$				
Hel-08	A2F	5′-ACATCTCAGAACTGGTCGGC-3′	58°; 1.5 mM	3	HEC 12	Alternative allele of *Hel-11* (CA10)	Flanagan *et al.* (2002)
	A2R	5′-CTCGATCAGCCGGTGATTAT-3′	$MgCl_2$				
Hel-02	B32F	5′-TCAAAATGTTGCAGACCGAG-3′	55°; 3.0 mM	2	HEE 7		Flanagan *et al.* (2002)
	B32R	5′-TGCACTTCATTGTAAGGCGT-3′	$MgCl_2$				
Hel-14	AAT4F	5′-GCACATTTACTTACACTAACGC-3′	53°; 1.5 mM	3	HEC 2	Alternative allele of *Hel-13* (CA13), Tobler *et al.* 2005	Flanagan *et al.* (2002)
	AAT4R	5′-ATTTGTTTCGAACGACTGCC-3′	$MgCl_2$				
He-CA-001	A25F	5′-CGGGACACAAAATGTGACTG-3′	58°; 3.0 mM	3	HEE 9[d]		Tobler *et al.* (2005)
	A25R	5′-AACTGGACGGTGGACGTTAG-3′	$MgCl_2$				
He-CA-002	CJ-MS18F	5′-ACGTCTGCGGTCTGGCTGTC-3′	56°; 1.5 mM	3	HEC Z		This study (DQ380225)
	CJ-MS18R	5′-TGGTAGGGAAGTAATGAAAC-3′	$MgCl_2$; BSA 0.8 mg/ml				
He-CA-003	CJ-MS32F	5′-AGCAAGATTGTCGCATGTCA-3′	54°; 1.5 mM	3	[a]	[e]	This study (DQ380226)
	CJ-MS32R	5′-ACGAAATGGAACCCAAAACA-3′	$MgCl_2$; BSA 0.8 mg/ml				
He-CA-004	CJ-MS37F	5′-TTGTAGTCGGATTTATGGCAAA-3′	56°; 1.5 mM	3	HEE 11		This study (DQ380227)
	CJ-MS37R	5′-GGTCCTTAGTCATGTCGCAAA-3′	$MgCl_2$; BSA 0.8 mg/ml				
He-CA-005	CJ-MS40F	5′-TGTCCTACATGGATACGGAGAA-3′	56°; 1.5 mM	3	HEC 12		This study (DQ380228)

(*continued*)

TABLE 2

(Continued)

Marker name	Primer name	Primer sequence	Reaction conditions	No. of alleles	Mapping group	Notes	Source (GenBank no.)
	CJ-MS40R	5′-CCAGCATCTTTGCCCCTTA-3′	$MgCl_2$; BSA 0.8 mg/ml				
Hm_06	CJ-MS44F	5′-AAATAGTGTGCGGCGGAATA-3′	54°: 1.5 mM	2	HEC 5[f]		Jiggins *et al.* (2005)
	CJ-MS44R	5′-TGGAGTAGAAATGCGGGTTTA-3′	$MgCl_2$; BSA 0.8 mg/ml				
He-CA-007	CJ-MS47F	5′-GCTACGAGCCTCACCTGAAC-3′	51°: 1.5 mM	4	[a]	[g]	This study (DQ380229)
	CJ-MS47R	5′-GACTAACGGCACCTCCACAC-3′	$MgCl_2$; BSA 0.8 mg/ml				
He-CA-008	CJ-MS60F	5′-CGCCACGACGGATAAAAAT-3′	56°: 1.5 mM	2	HEC 12		This study (DQ380230)
	CJ-MS60R	5′-TTAAACCTCAACCGCACTTT-3′	$MgCl_2$; BSA 0.8 mg/ml				

NA, not available.
[a] The locus did not map. See Materials and Methods for details.
[b] Loosely associated with LG19 but too many obligate recombinants to map.
[c] Unable to consistently score.
[d] MI grouped only.
[e] This BI locus was not converted to MI because there were too many obligate double recombinants in the BI analysis.
[f] FI grouped only.
[g] This locus only had MI alleles and did not group at this step.

In step two, we compared each chromosome print with BI AFLPs as well as codominant anchor loci with segregation ratios of 1:1:1:1 or 1:2:1. Applying JoinMap 3.0 to an intercross design, we identified loci that grouped at LOD 5.0 or higher with each chromosome print (in a few cases codominant markers grouped at LOD 4.0 and were included in groups for subsequent verification). Because the genetic model employed by JoinMap assumes crossing over in both males and females, which was not so in our case, new groups were individually examined to verify linkage with a unique chromosome print (see Results), check phase, and to identify forbidden recombinants (Shi *et al.* 1995), defined as offspring genotypes impossible without crossing over in females unless there were scoring errors. In our analysis we accept a small amount of scoring error and retained BI loci with five or fewer forbidden recombinants that have a probability of $P < 0.007$ or lower of being unlinked under the hypothesis of no scoring error (see Jiggins *et al.* 2005). The BI AFLP loci associated with a particular chromosome print were labeled by linkage group (LG-#). We then extracted the MI component from the BI AFLP scores (*i.e.*, following only AFLP bands inherited from the father) by censoring the scores that included AFLP bands inherited from the mother (Jiggins *et al.* 2005). For the sex chromosome, Z, male offspring are always positive for BI AFLPs and the recombinant analysis is limited to female offspring segregating MI markers on Z (Jiggins *et al.* 2005).

In the third and final step, the censored BI markers (tagged with LG-#) were combined with MI AFLPs as well as codominant anchor markers recoded to show only the MI allele (see the BI → MI allele designation). Linkage groups were assembled at LOD 3.0 or greater and identified by one or more shared LG-# tagged AFLPs (Jiggins *et al.* 2005). All LODs to this point were calculated utilizing Joinmap 3.0. For final map construction, the most likely order and spacing of markers on a chromosome was determined utilizing Mapmaker 3.0 applied to a backcross design (Lincoln *et al.* 1987). First, all markers within a linkage group were converted to the same linkage phase and compared using Mapmaker's "join haplotypes" command. Haplotypes were consolidated over missing data by grouping MI markers with identical genotypes (derived from either phase) or censored BI markers (in the same original linkage phase) as a haplotype in Mapmaker. Censored BI markers originally in the opposite linkage phase may form spurious haplotype groups since the censoring step creates marker sets of different complementary individuals for each phase. Haplotypes including these latter markers were removed unless both joined to an MI locus of either linkage phase. Linkage group memberships of these haplotypes and the remaining markers were reverified using Mapmaker's "assign" command.

To find the most likely order for linkage groups with eight or fewer unique loci (single markers and haplotypes), we used Mapmaker's "compare" command to examine all possible orders. For larger linkage groups we automated the construction of a preliminary scaffold of five or fewer markers utilizing the "order" command. Following standard Mapmaker methods (Lincoln *et al.* 1987) additional markers were inserted into the scaffold in order of their impact on the LOD score (utilizing cutoffs in descending order of LOD 3.0, LOD 2.0, LOD 1.0, and <LOD 1.0) until the likelihood of the resulting map was maximized. Although these LOD values are not normally saved during the map-building process, we utilized Mapmaker scripts to keep track of markers mapping at each LOD value (see Figure 2). In all cases we preferentially initialized our scaffold with MI AFLP loci, which had the highest number of scored individuals and the highest impact on the likelihood. All markers mapping to a unique interval

TABLE 3

Summary of single copy nuclear loci used in this study

Name	Primer name	Primer sequence	Intron[a]	PCR reaction conditions[b]	No. of segregating alleles	Scoring method[c]	Mapped in *H. erato*	Mapped in *H. melpomene*	Source
Apterous (*ap*)	Ap-F(35)	5′-TGAATCCTGAATACCTGGAGA-3′	X	Inconsistent amplification	NA	NA		HMEL (Z)	Jiggins *et al.* (2005)
	Ap-R(357)	5′-CTTTTCCGCCATTTTGTTCTC-3′							
Cubitus interruptus (*ci*)	Ci-F(85)	5′-AACACAGATCACATACACGCA-3′	X	53°; 2.5 mM MgCl; 0.8 mg/ml BSA	3	SNuPE	HEC 3	HMEL 18	Tobler *et al.* (2005)
	Ci-R(416)	5′-TGTATCTTTTAGTGCAACCCG-3′							
Dopa-decarboxylase (*ddc*)	Ddc-F(50)	5′-CAGAGGGTCAAGGAACAGCAC-3′	X	60°; 2.5 mM MgCl; 0.8 mg/ml BSA	NA	NA	No segregating variation	HMEL 1	Tobler *et al.* (2005)
	Ddc-R(402)	5′-TCATGAGGTAGCGGTACTCGG-3′							
Decapentaplegic (*dpp*)	Dpp-F(34)	5′-AGAGAACGTGGCGAGACACTG-3′		52°; 2.5 mM MgCl; no BSA	2	SNuPE	HEC 14	HMEL 19	Tobler *et al.* (2005)
	Dpp-R(327)	5′-GAGGAAAGTTGCGTAGGAACG-3′							
Wingless (*wg*)	Wg-F	5′-CCCAGTTTTAGATCTGTCG-3′		50°; 2.5 mM MgCl; no BSA	4	SNuPE	HEC 14		Brower (1996)
	Wg-R	5′-TCTCGGTCCGGTATCCGCG-3′							
Triose-phosphate isomerase (*tpi*)	Tpi-F	5′-GGTCACTCTGAAAGGAGAACCATCTT-3′	X	50°; 2.5 mM MgCl; no BSA	3	SNuPE	HEC Z	HMEL Z	Beltrán *et al.* (2002)
	Tpi-R	5′-CACAACATTTGCCCAGTTGTTGCCAA-3′							
Mannose phosphate isomerase (*Mpi*)	Mpi-F	5′-TTTAAGGTGCTCTATATAAGRAARGC-3′	X	50°; 2.5 mM MgCl; no BSA	3	RFLP/*Alu*I (NEB)	HEC 5	HMEL 3	Beltrán *et al.* (2002)
	Mpi-R	5′-TTCTGGTTTGTGATTTGGATCYTTRTA-3′							
Patched (*ptc*)	Ptc-F(7)	5′-CTCCGAAGAAGGTCTGCCGCAAG-3′	X	53°; 2.5 mM MgCl; no BSA	4	SNuPE	HEE 6	HMEL 10	Jiggins *et al.* (2005)
	Ptc-R(364)	5′-AATTCGTGCTCGTCGTATTTTC-3′							
kyurene 3-hydroxylase (*cinnibar*)	Cinn-F(23-bob)	5′-AGGATTGTTCGTGGACCG-3′	X	50°; 2.5 mM MgCl; no BSA	4	SNuPE	HEE 15		This study (DQ380223)
	Cinn-R(376-bob)	5′-GCATCTCTCCATCTTTTGCC-3′							
Long-wavelength opsin (*opsin*)	Opsin-5′RACERH1	5′-TGGTTACAATAGGGCTGA-3′		Inconsistent amplification	NA	NA		HMEL 11	Jiggins *et al.* (2005)
	Opsin-RLWFD4	5′-ACAAAAATCAATGGGAGAGTA-3′							
Elongation Factor 1α (*EF1a*)	EF1H-F	5′-GAGAAGGAAGCCCAGGAAAT-3′		52°; 2.5 mM MgCl; no BSA	3	SNuPE	HEE 6	HMEL 10	Jiggins *et al.* (2005)
	EF1H-R	5′-CCTTGACRGACACGTTCTTT-3′							
Hedgehog (*hh*)	Hh-F(38)	5′-AAGGAAAAACTGAATACGCTGGC-3′		52°; 2.5 mM MgCl; no BSA	3	RFLP/*Sau*96I and *Sau* 3AI[d]	HEC 10		This study (DQ380223)
	Hh-R(206)	5′-CGAGACGCGCCAACTTTCC-3′							
Ribosomal protein L5 (*RpL5*)	RpL5-F(44)	5′-TCCGACTTTCAAACAAGGATG-3′	X	52°; 2.5 mM MgCl; no BSA	4	SNuPE	HEE 7	HMEL 11	Jiggins *et al.* (2005)
	RpL5-R(499)	5′-TGAAGACCGAAGATGTGTGC-3′							
Ribosomal protein S5 (*RpS5*)	RpS5-F(31)	5′-GGTTGAGGAAAACTGGAACG-3′		52°; 2.5 mM MgCl; no BSA	3	SNuPE	HEE 7	HMEL 11	Jiggins *et al.* (2005)
	RpS5-R(490)	5′-TACGGCTTGACGACGTACTG-3′							

(*continued*)

TABLE 3

(Continued)

Name	Primer name	Primer sequence	Intron[a]	PCR reaction conditions[b]	No. of segregating alleles	Scoring method[c]	Mapped in *H. erato*	Mapped in *H. melpomene*	Source
Ribosomal protein S8 (*RpS8*)	RpS8-F(56)	5′-GCCCATTCGTAAGAAGAGGAA-3′	X	52°; 2.5 mM MgCl; no BSA	3	RFLP/*Dpn*II (NEB)	HEE 7	HMEL 11	Jiggins *et al.* (2005)
	RpS8-R(571)	5′-CAAGGACATAGCCATCAGCA-3′							
Ribosomal protein S9 (*RpS9*)	RpS9-F(12)	5′-GCCATCATGGTGAACAACAG-3′	X	52°; 2.5 mM MgCl; no BSA	2	Size polymorphism	HEE 8	HMEL 14	Jiggins *et al.* (2005)
	RpS9-R(493)	5′-TCAATGTGCTTGCCAGAGTC-3′							
Ribosomal protein L3 (*RpL3*)	RpL3-F(59)	5′-CCGTCATCGTGGTAAAGTGA-3′	X	52°; 2.5 mM MgCl; no BSA	2	SNuPE	HEC 4	HMEL 1	Jiggins *et al.* (2005)
	RpL3-R(537)	5′-TCTCCATGATATGGGCCTTC-3′							
Ribosomal protein L10a (*RpL10a*)	RpL10a-F(192)	5′-GTACATTCCCAGGCCAAAAA-3′	X	52°; 2.5 mM MgCl; no BSA	3	Size polymorphism[e]	HEE 7	HMEL 11	Jiggins *et al.* (2005)
	RpL10a-R(574)	5′-TTCTGTGCCAACTCATCAGG-3′							
Ribosomal protein L11 (*RpL11*)	RpL11-F(138)	5′-CTGTGTCGGTGAATCTGGTG-3′		Inconsistent amplification	NA	NA		HMEL 5	Jiggins *et al.* (2005)
	RpL11-R(571)	5′-CTGTTGGAACCACTTCATGG-3′							
Ribosomal protein L19 (*RpL19*)	RpL19-F(131)	5′-CCCGACAGAACATCCGTAAG-3′		Inconsistent amplification	NA	NA		HMEL 10	Jiggins *et al.* (2005)
	RpL19-R(529)	5′-CGGGCTTCCTTCACTCTGT-3′							
Ribosomal protein P0 (*RpP0*)	RpP0-F(142)	5′-ACCCAAAATGTTTCATCGTG-3′	X	52°; 2.5 mM MgCl; no BSA	3	Size polymorphism	HEE 7	HMEL 11	Jiggins *et al.* (2005)
	RpP0-R(565)	5′-TCACCAGGCTTCAAGATGTG-3′							

NA, unable to score the locus in the mapping family.

[a] An X indicates an intron was present.

[b] Annealing temperature, [MgCl], [BSA].

[c] Including RFLP enzyme.

[d] First digestion with *Sau*96I allowed discrimination of two of four possible offspring genotypes. To distinguish individuals for which the first digestion was not informative, the other two genotypes were separated by a second digestion with *Sau*3AI.

[e] Scored directly from PCR amplification (father 240 had a null allele that never amplified) leading to three distinguishable genotypes.

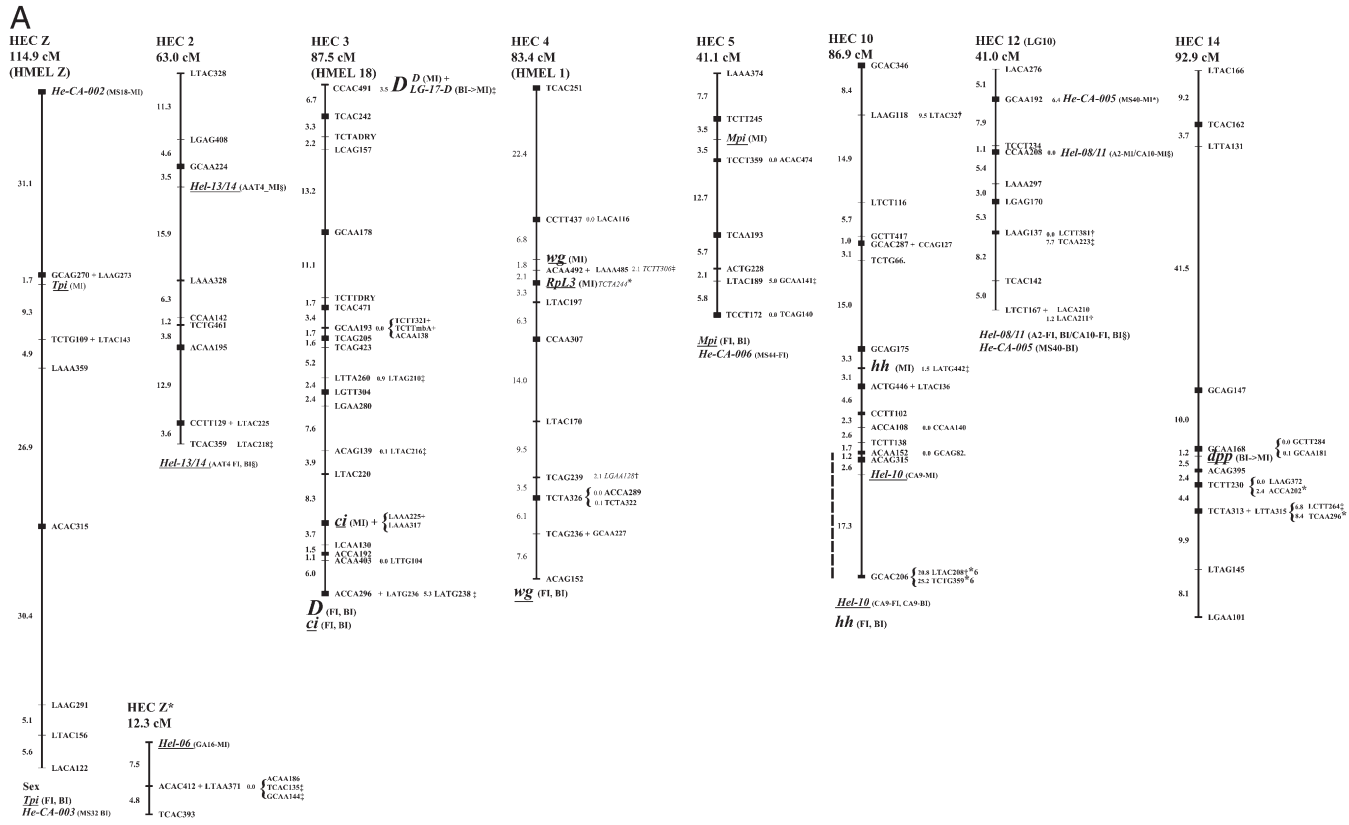

FIGURE 2.—Integrated genetic map for *H. erato etylus* and *H. himera*. Linkage groups with codominant anchor loci that allow between-study comparisons are named within a species by the race and linkage group they were first identified with, starting with Z (*e.g.*, the sex chromosome in *H. erato cyrbia* is HEC *Z*; TOBLER *et al.* 2005). (A) Groups homologous to *H. erato cyrbia* HEC 2, 3, 4, 5, 10, 12, and 14. (B) In this study we recognize further linkage groups *H. erato etylus* (HEE 6, 7, 8, 9, 11, 13, and 15) in total identifying 15 of 21 *H. erato* linkage groups. Tentative homology to *H. melpomene* is indicated by code HMEL and linkage group number from JIGGINS *et al.* (2005). (C) *H. erato etylus* groups *a–f* do not include any anchor loci and hence are not easily portable to other studies. A–C are drawn to different scales. On the map the L-# prefix signifies BI markers that segregated with a unique chromosome print in the BI analysis and were subsequently mapped with the band-positive allele inherited from the father. AFLP marker names are read as follows: L prefix markers, such as LAAA374, indicate a BI censored marker **L***G1_Eco-C***A**_*Mse-C***AA_374** base pairs where only boldface (non-italicized) letters are shown. Non-L prefix markers indicate MI markers and include the first letter of the *Eco*RI primer and all three bases of the *Mse*I primer, such as: *Eco-C***T**_*Mse-***CTT_245** for TCTT245. Codominant marker names include segregation pattern in parentheses (FI, BI, BI → MI, MI, see supplemental Appendix at http://www.genetics.org/supplemental/ for expanded marker names for all loci). Map position lines of variable thickness indicate framework markers mapping to unique intervals at >LOD 3.0 (thickest), >LOD 2.0 (medium), >LOD 1.0 (thin), <LOD 1.0 (thinnest). Nonframework markers are found to the right of framework markers. Markers joined with a + symbol form identical haplotypes with no recombination. Haldane cM values of 0.0–0.1 to the right of framework markers indicate the markers so joined are indistinguishable from framework markers at the 1% *a priori* error rate. Remaining markers to the right of framework markers are placed on the map but do not contribute to its order, length, or likelihood (see MATERIALS AND METHODS and RESULTS). Centimorgan values >0.1 indicate most likely placement below for one of these nonframework markers, no centimorgan values indicate marker could place on either side of framework marker. Italics indicate placements with errors. A ‡ symbol indicates a nonframework marker that places in more than one interval. A † symbol indicates a nonframework marker had ≥6 forbidden recombinants for a BI locus but may be part of the linkage group given other data. An * symbol indicates a nonframework marker with a segregation distortion of $P < 0.02$. Arrows (either ↑ or ↓) indicate marker placed off respective end of chromosome at given distance. Microsatellites indicated by a § symbol were mapped with alternative alleles of the same locus entering in different linkage phases (both shown, see Table 2 and supplemental Appendix for details, http://www.genetics.org/supplemental/). Markers below each map are likely members of the linkage group (on the basis of FI, BI, or LOD association data) but do not map in a 1:1 analysis. Dashed line at bottom of HEC 10 represents the only segment whose maximum likelihood order was flipped with respect to remaining markers when the error detection switch was turned off in Mapmaker. We also placed a small group of four ALFP loci at the bottom of HEE 7 that distantly associated with this group and were not used to calculate map length.

were considered part of the map's framework. Censored BI loci have half or fewer genotypes than MI markers and occasionally could not be mapped to a unique framework position relative to one or more flanking markers. These markers were placed on the map using the "place" command in Mapmaker in their most likely position to represent this information visually (Figure 2). As a quality control measure we also verified that the approximate method to handle larger linkage groups, based on the order command, gave identical results to the compare command for the four autosomal groups with eight or fewer loci as well as for all subsets of eight loci of larger linkage groups run for test purposes.

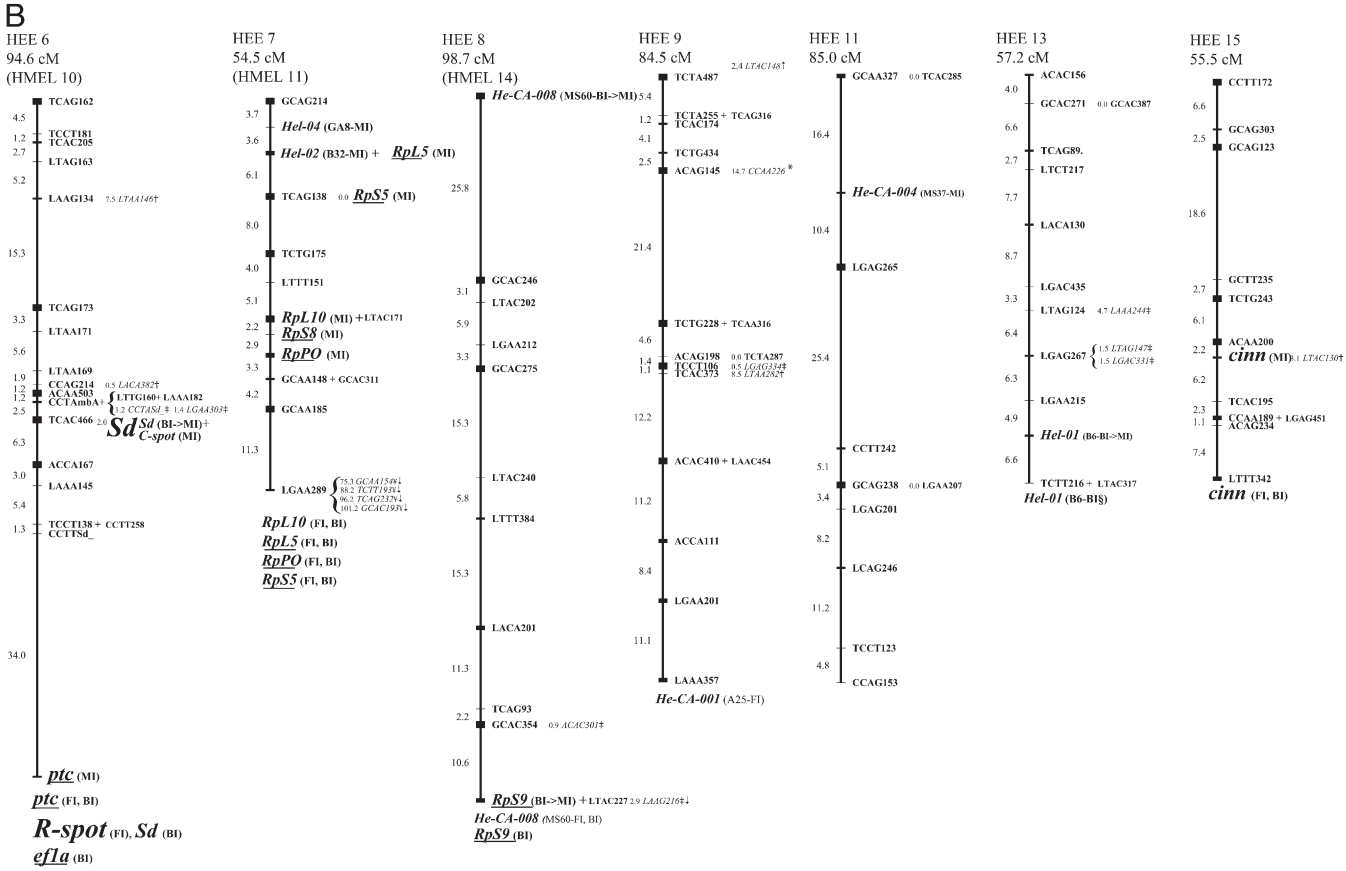

FIGURE 2.—*Continued.*

In summary, these methods allow integration of these three types of markers into a single unified map. Final linkage groups were designated HEC # where homology between our preliminary mapping study of *H. erato cyrbia* and *H. himera* (TOBLER *et al.* 2005) could be identified. Remaining linkage groups containing one or more codominant anchor loci are given a number in the same series with an *H. erato etylus* (HEE #) designation to highlight the fact that although identical in the present study, homology with previous HEC groups has not been ascertained. Finally, any remaining linkage groups without an anchor locus are given a letter, indicating that homology for these linkage groups is not easily portable to future studies.

To explore the effect of any potential residual genotyping errors we ran all of the final Mapmaker analyses both with and without error detection (LINCOLN and LANDER 1992). Final genetic distances are expressed in terms of uncorrected Haldane centimorgans (cM) with error detection function left on, both recognizing unresolved genotyping errors and allowing a direct comparison with JIGGINS *et al.* (2005).

Development of additional AFLP markers linked to color pattern: We scanned for additional bands linked to color pattern loci by running five primer combinations (Table 1 legend) on the high-resolution LI-COR AFLP system with individuals presorted by their color pattern genotype (see TOBLER *et al.* 2005 for LI-COR methods). Specifically, we loaded groups of individuals with the same homozygous genotype at a single color pattern locus on adjacent gel lanes allowing the quick visual identification of bands *cis* to one of the alternate alleles for a given color pattern. Perfectly linked loci in these multilane metabulks will form a continuous band corresponding to one or the other group of adjacent homozygous individuals. These instantly recognizable bands were reverified by repeated genotyping of the entire brood in original plate order. The latter genotypes were used for mapping (see Figure 2 and supplemental Appendix at http://www.genetics.org/supplemental/). This method differs from bulked segregant analysis (MICHELMORE *et al.* 1991) in that the individuals in the genotypic groups are not added together or bulked into the same sample tube or well.

RESULTS

Phenotypic variation: Wing pattern variation across the 88 individuals in this cross was easily understood according to the classic methodology of SHEPPARD *et al.* (1985) and assuming allelic variation at both the *D* and *Sd* locus (Figure 1). At the *D* locus, both parental F_1's (PR269 and PR240) had both the orange Dennis and rays characteristic of *H. erato etylus* with the rays broadened at the base to blend into the dorsal hindwing bar of *H. himera* (Figure 1B, hindwings). At the *Sd* locus, parental F_1's had solid black dorsal forewings because alternative alleles that encode for proximal Sd^{et} *vs.* distal Sd^{hi} melanin together completely obscure the yellow bands (Figure 1B) also seen in heterozygous F_2 offspring (Figure 1C, middle column). The lack of strong epistasis and clear codominance of alleles at both *D* and

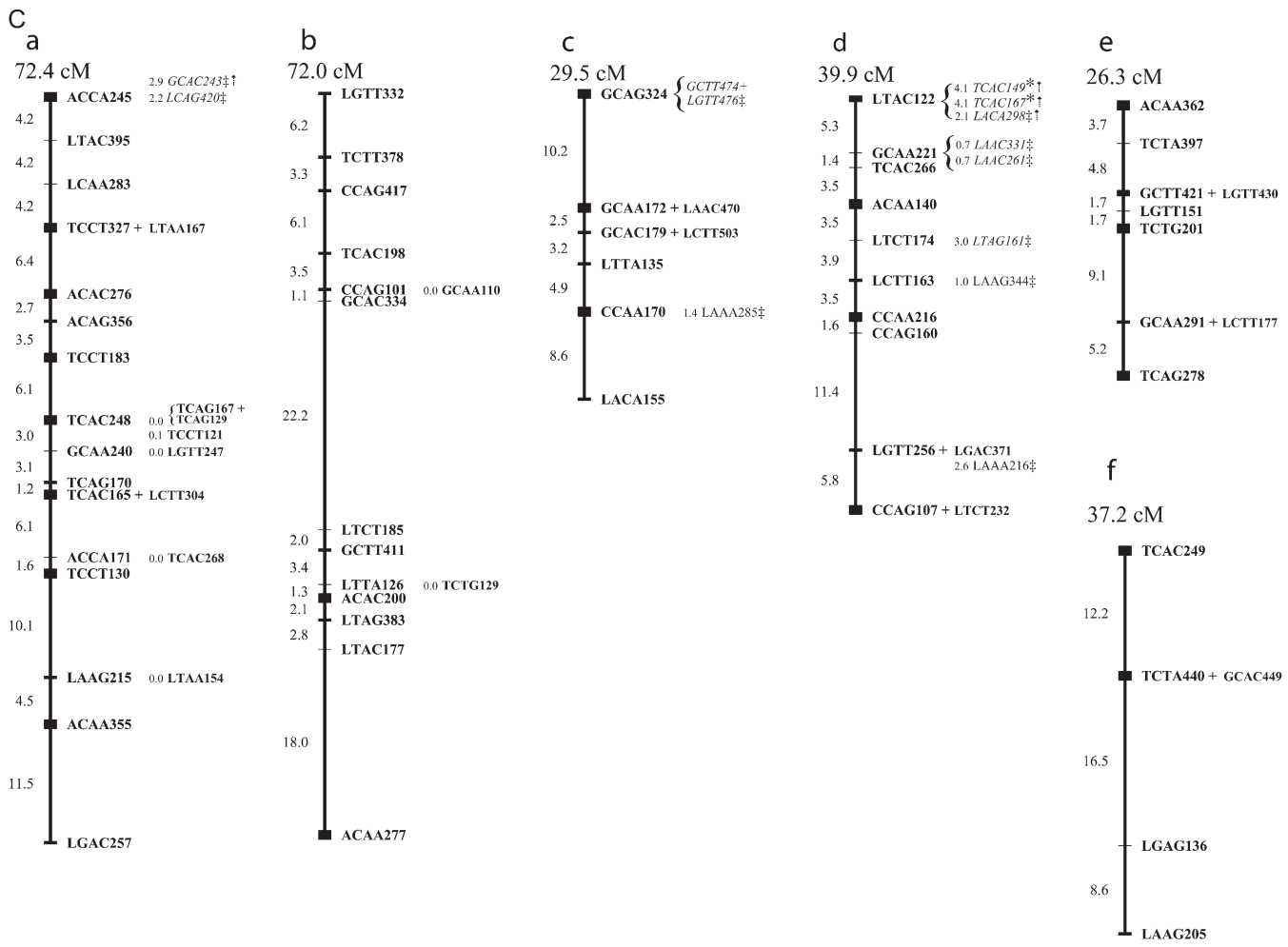

FIGURE 2.—*Continued.*

Sd was evident from the nine easily distinguishable phenotypes among the F_2 progeny (Figure 1C). The forewing Dennis and hindwing rays of *H. erato etylus* were always inherited together in this and other F_2 crosses of *H. erato etylus* and *H. himera*, consistent with a single locus hypothesis. Further, these pattern elements and the hindwing bar of *H. himera* segregated in a clear Mendelian fashion (21:46:21, $G_2 = 0.18$, $P = 0.913$) and suggested that the phenotypic effects are controlled by allelic variation at the same locus. Determining the genotype of individuals at the *Sd* locus was similarly straightforward. Although more distorted, the phenotypes segregated as expected for a single di-allelic codominant locus (16:54:18, $G_2 = 4.70$, $P = 0.095$). These two codominant loci segregate independently ($G_8 = 11.55$, $P = 0.172$).

In addition, individuals heterozygous at the *Sd* locus also showed variation (presence/absence) of small yellow spots on the dorsal and ventral forewing (Figure 1). Some individuals possessed a small spot in the proximal wing cell (the discal cell spot, or c-spot, Figure 1D), whereas others showed a spot between wing veins R2 and R1 sometimes extending to the SC vein (the r-spot Figure 1D). The c-spot and r-spot never co-occur in the same individual and segregate as alternate alleles at a single locus expressed in a 1:1 fashion (c-spot: present 39:absent 49, $G_1 = 1.14$, $P = 0.29$; r-spot: present 45:absent 43, $G_1 = 0.05$, $P = 0.83$). Further, the c-spot has MI phenotypic effects and shows a segregation pattern that is identical with *Sd*. These identical genotypes strongly suggest that the c-spot is controlled by an alternative allele of the *H. erato etylus Sd* locus. The r-spot is also likely to be encoded by *Sd* (this FI phenotype grouped with the *Sd* locus by chromosome print), but in this cross we were unable to map r-spot since it does not display MI phenotypic effects. In Heliconius crosses, alleles of loci coding for the presence of melanic scales at a given wing position are generally dominant to alleles for yellow scales (GILBERT *et al.* 1988). In this cross, individuals with all dark wings reveal that, similar to the *Sd* locus, the two *H. erato etylus*-derived spot alleles have codominant effects (Figure 1). This interpretation leads to a hypothesized 1:1:1:1 ratio for the phenotypes: no spots (all dark wings):r-spot: c-spot:no spots (all yellow *H. himera* forewing, $G_3 = 1.18$, $P = 0.76$).

Markers: From the 20 *Eco*RI-C*N*/*Mse*I-C*NN* (where *N* represents variable nucleotides in the selective PCR amplification) AFLP primer combinations examined (Table 1), we scored 191 maternally inherited 1:1 loci (FI), 182 loci present in both the mother and father (BI), and 190 paternally inherited 1:1 loci (MI). Of these 564 loci, 29 of 382 1:1 loci (or ~8%) had statistically significant segregation distortion (G test, $P < 0.05$) while 24 of 182 (or ~13%) of the BI loci showed segregation distortion (G test, $P < 0.05$). In addition, we were successful in scoring 18 microsatellite loci (out of 19 attempted, Table 2) that produced as many as seven alleles in the grandparents (range two to seven) and four in the parents (Table 2). By following different alleles inherited from either the mother or the father, or both, we were able to score the same microsatellite loci with different inheritance patterns (7 as 1:1 FI, 9 as codominant loci with three genotypes, and 10 as 1:1 MI loci). In addition to codominant microsatellites, we successfully genotyped 16 of the 21 SCNL screened, including 2 (*Hh*, *Cinn*) first reported here (Table 3). These SCNL had a range of 2–4 alleles in the parents, and depending on cross type, several could be scored with multiple segregation patterns (12 as 1:1 FI, 14 as codominant, and 14 as 1:1 MI loci). Locus details, including primer sequence, the number of segregating alleles, and comparison to previous mapping work in Heliconius, are given in Tables 1–3.

Sources of variation: To determine the proportion of markers entering the cross from either the *H. erato etylus* or the *H. himera* side, we assessed whether a given dominant AFLP locus was absent, present as a polymorphism, or likely arose as a fixed difference between *H. erato etylus* or *H. himera* grandparents by carefully following genotypes of the progenitors, linkage phases of the loci, and segregation patterns of the offspring. For the 477 AFLP bands for which linkage phase of the grandparents could be ascertained with certainty, 168 were monomorphic negative (band always absent), 261 were polymorphic, and 41 were probably fixed (band positive) in *H erato etylus* (due to the dominance of AFLP loci it is impossible to ascertain with certainty whether or not a given locus was monomorphic in the grandparents of either species). This contrasts with 244 monomorphic negative, 130 polymorphic, and 96 probably fixed (band positive) loci for *H. himera*. A further 7 loci may have been fixed in either one but not both species. Thus most of the variation derived from bands unique to *H. erato etylus* (~52%) *vs.* bands unique to *H. himera* (36% of the variation); however, in the latter a higher number of these bands were likely monomorphic within the *H. himera* grandparents (20%) *vs.* the *H. erato etylus* grandparents (9%).

The codominant anchor loci gave largely the same picture and *H. erato etylus* was consistently more variable than *H. himera*. For the 18 microsatellites and 1 SCNL (*Ci*) for which grandparental genotypes were known 17 were polymorphic in *H. erato etylus*. This contrasts with *H. himera* where 7 loci were monomorphic and 12 were polymorphic. Although both species had a range of one to four codominant alleles per locus, *H. erato etylus* had an average of 2.5 alleles per locus, while *H. himera* had an average of 1.9 alleles per locus. Overall, 8 loci had unique alleles in one genetic background, while 9 shared one allele and 2 shared two alleles between each species.

Chromosome prints and marker error estimation: We assessed the level of genotyping error using the 191 FI polymorphic AFLP loci. All of these loci were assigned to 1 of 21 linkage groups, matching the expected number of chromosomes on the basis of early cytogenetic work (Brown *et al.* 1992; Suomalainen *et al.* 1971, 1973; Turner and Smiley 1975) and recently confirmed for *H. erato* and *H. himera* (Tobler *et al.* 2005) and for *H. melpomene* (Jiggins *et al.* 2005). Linkage groups included as many as 15 and as few as 4 FI AFLP markers (Table 4). In addition to AFLP loci, we successfully grouped six of seven microsatellites, 11 of 12 SCNL, and the one color pattern (r-spot) that could be scored in a 1:1 FI manner (see supplemental Appendix at http://www.genetics.org/supplemental/). Anchor loci *He-CA-005* and *EF1a* did not group at this step because they had many missing genotypes due to amplification and scoring difficulties.

The nonrecombining female chromosomes permit the unambiguous identification of forbidden recombinants providing an ideal standard against which to assess residual genotyping error. Within the FI markers, the number of forbidden recombinants ranged from 0 to 21 per locus (median 1, mean 3) and 0 to 16 per individual (median 6, mean 6.3) for a total of 550 of the 16,808 genotypes (or 3%) showing a genotyping error from the 88 offspring of the brood. However, unlike Jiggins *et al.* (2005), all FI AFLP loci without exception grouped at LOD 8.0; in addition, nearly 80% of the scored loci showed fewer than five forbidden recombinants, indicating that most loci were reliable.

Association of chromosome print with BI markers: Nearly all of the BI markers (182 AFLP, 9 microsatellites, and 14 SCNL) formed linkage at LOD 5.0 with each other and a unique chromosome print and thus were considered syntenic to the FI linkage groups. The LOD 5.0 grouping left only 22 ungrouped BI AFLP markers (9 were excluded prior to this step because of high segregation distortion, χ^2 tests in Joinmap 3.0, $P < 0.01$). Of the 22 ungrouped loci, 7 grouped with a single chromosome print at LOD 4.0 and 4 grouped with a single chromosome print at LOD 3.0. In addition, one microsatellite, *He-CA-005* (MS40), not linked in the FI analysis, grouped with LG10 at LOD 4.0 (see supplemental Appendix at http://www.genetics.org/supplemental/). In the absence of scoring errors, across 88 offspring an unlinked locus would have ~one-eighth, or 11, forbidden recombinants on average (Jiggins *et al.*

TABLE 4

Summary of marker data for *H. erato etylus* linkage groups identified in the present study

H. erato linkage group	Final no. of AFLP markers				SCNL	Color pattern	Microsatellites	Final framework marker no.	Size (cM)
	FI	BI	BI → MI	MI[a]					
Z	4	9	6	3	*Tpi* (FI, BI, MI)	—	*He-CA-003* (MS32-BI), *He-CA-002* (MS18-MI)	9	114.9
Z*[b]	—	—	1	5	—	—	*Hel-06* (GA16-MI)	3	12.3
HEC 2	10	7	5	6	—	—	*Hel-14* (AAT4-FI, BI, MI)	10	63.0
HEC 3	9	16	15	12	*ci* (FI, BI, MI)	*D* locus: D (BI), D (BI→MI)	—	20	87.5
HEC 4	14	6	5	13	*wg* (FI, BI, MI), *RpL3* (MI)	—	—	12	83.4
HEC 5	13	3	2	8	*Mpi* (FI, BI, MI)	—	*Hm06* (MS44-FI)	8	41.1
HEC 10	7	8	6	16	*hh* (FI, BI, MI)	—	*Hel-10* (CA9- FI, BI, MI)	16	86.9
HEC 12	6	8	8	5	—	—	*Hel-11* (CA10- FI, BI, MI), *He-CA-005* (MS40-BI)	9	41.0
HEC 14	12	7	7	10	*dpp* (BI, BI→MI)	—	—	11	92.9
HEE 6	7	12	10	11	*ptc* (FI, BI, MI), *ef1a* (BI)	*Sd* locus: r-spot (FI), *Sd* (BI), c-spot (MI)	—	17	94.6
HEE 7	5	4	3	10	*RpL5*, *RpS5*, *RpL10a*, *RpS8*, *RpPO* (FI, BI, MI)	—	*Hel-02* (B32-MI), *Hel-04* (GA8-MI)	12	54.5
HEE 8	6	12	7	5	*RpS9* (BI)	—	*He-CA-008* (MS60- BI, BI→MI)	11	98.7
HEE 9	13	8	6	15	—	—	*He-CA-001* (A25-FI)	13	84.5
HEE 11	7	7	4	6	—	—	*He-CA-004* (MS37-MI)	9	85.0
HEE 13	4	10	10	5	—	—	*Hel-01* (B6- BI, MI), *Hel-07* (GA19-BI)[b]	11	57.2
HEE 15	11	4	3	9	*cinn* (FI, BI)	—	—	11	55.5
a	9	9	9	16	—	—	—	16	72.4
b	6	5	5	10	—	—	—	13	72.0
c	11	6	7	5	—	—	—	6	29.5
d	15	12	12	8	—	—	—	10	39.9
e	13	5	3	6	—	—	—	7	26.3
f	9	2	2	3	—	—	—	4	37.2
Total[d]	191	160	136	186				238	1430.3

[a] Mapped or placed in the MI data.

[b] Two linkage groups with Z markers form in the MI data.

[c] These two microsatellite markers on Z in first *H. e. cyrbia* map (Tobler *et al.* 2005).

[d] This excludes 22 BI, 11 converted BI to MI and 2 MI markers not grouping as well as 16 converted BI to MI and 2 MI markers that did not map (see supplemental Appendix for details; http://www.genetics.org/supplemental/).

2005). As a conservative measure we retained loci with 5 or fewer forbidden recombinants grouping at LOD 5.0 with a unique chromosome print (see MATERIALS AND METHODS) and identified 16 loci with ≥6 forbidden recombinants. Unlike JIGGINS *et al.* (2005) we did not categorically eliminate these markers, but if they consistently associated with other LG-# markers from the same group before and after censoring, they were placed on the framework map without affecting map order, length, or likelihood (see markers with a dagger symbol denoting tentative membership, Figure 2). We converted the 167 remaining BI markers (163 BI AFLP markers, 2 microsatellites, and 2 SCNL) to 1:1 loci following JIGGINS *et al.* (2005). Subsequently, the predicted 1:1 segregation ratio for the markers was tested.

Mapping of MI markers: Our final MI data set consisted of 391 loci, including the 163 censored BI loci and 228 MI loci (198 AFLP markers, 14 microsatellites, and 16 SCNL) segregating in a 1:1 MI fashion. Of these markers, 7% show some segregation distortion at a $P < 0.05$. Of the 391 loci 355 were associated with a single linkage group (both *D* and *Sd* also associated at this step). An additional 9 censored AFLP loci, although grouping with other MI loci, were removed from the map because of inconsistent grouping between BI and MI scorings. A further 9 (5 censored AFLPs, 1 MI AFLP, and 1 microsatellite locus), although grouping with other MI loci, were removed from the map because of an excess of recombinants (see supplemental Appendix at http://www.genetics.org/supplemental/). A final 18 loci did not group at the final mapping step [3 MI AFLPs, 11 converted BI to MI AFLPs, as well as a microsatellite anchor locus *HE-CA-007* and a SCNL (*EF1a*) due to missing genotypes, amplification, and scoring difficulties; see supplemental Appendix at http://www.genetics.org/supplemental/].

Despite some residual genotyping error, estimated linkage group size and map order was relatively stable. First, average linkage group length increased asymptotically 76, 83, and 96% with markers added to the map for LOD cutoffs 3.0, 2.0, and 1.0, respectively. To assess the effect of genotyping error on marker order, we compared maps generated with the error detection algorithm in Mapmaker both enabled and disabled. As a compromise between the observed 3% overall error rate (per genotype) and low (0.5%) median error rate per locus in the FI data we set the threshold for Mapmaker's error detection function at 1%. Maps calculated with both options were very similar; the largest difference was the inversion of a single group of four markers on HEC 10 (Figure 2). Furthermore, the remaining differences were due to markers considered statistically indistinguishable with error detection on (*e.g.*, 0.0 or 0.1 cM designation in Figure 2 and supplemental Appendix, http://www.genetics.org/supplemental/) that mapped directly adjacent to markers that map to a unique position with error detection off.

The final map contained a total of 238 (range 4–20) framework markers (*i.e.*, those that map to a unique position) spread across 21 linkage groups (Figure 2). In addition, 38 loci cosegregated completely and thus formed a haplotype with a framework marker, and 30 markers were statistically indistinguishable from framework markers within the 1% error rate. We also placed an additional 49 nonframework markers on the framework map in their most likely position (Figure 2). Interestingly, although 21 chromosome prints including the sex chromosome (Z) were identifiable with the FI and the BI data, there were two separate linkage groups associated with the sex chromosome Z in the MI analysis (Figure 2, see below).

The overall size of the final map spanned 1430 Haldane cM when calculated with the error detection function in Mapmaker turned on. (With the error detection switch turned off it was predictably larger, at 1945 cM.) In general, the percentage of unique markers mapping at each LOD cutoff (~76–78%) remained steady, yet the number of centimorgans gained for each new unique marker decreased at each LOD cutoff as expected for a nearly saturated map: 11.3 cM/marker for the first 93 markers (>LOD 3.0), 6.3 cM/marker for the next 20 (>LOD 2.0), 3.9 cM/marker for the next 44 markers (>LOD 1.0), and 1.1 cM/marker for the last 80 markers. This pattern suggests that additional mapping effort on the same brood will not appreciably increase map resolution. Furthermore, given the residual genotyping error with AFLPs and the other loci in this study, increasing marker number would add little information but it would expand map size.

The distribution of the number of markers per linkage group and the intervals between markers across linkage groups both for FI and MI loci fit a uniform distribution suggesting that intermarker distances are randomly spaced across the genome (Kolmogorov–Smirnov Test against a uniform distribution, $KS = 0.112$, $P = 0.91$ for MI mapping intervals). Nonetheless, there was a high variation in the size of linkage groups indicated by both the number of markers in the chromosome prints and the map distance (Table 4). Autosomes had a minimum LG size of 26.3 cM and maximum of 98.7 cM, and the average distance between markers was 5.1 cM (median 5.1). Relative to this mean, three linkage groups appeared to be outliers. Group f had only 4 markers but had a high average of 12.4 cM/marker. In addition, the two linkage groups associated with the sex chromosome Z had apparently anomalous marker distributions. HEC Z (114.9 cM) had 9 framework markers and the highest average intermarker distance of 14.4 markers per cM. On the other hand, the extra group associated with the sex chromosome Z* (12.4 cM) has 6 markers and only 2.4 cM per marker.

All of the codominant anchor loci were mapped, with the exception of *EF1a* (which grouped with HEE 6 in the

BI data) and *He-CA-007*. Eight of the 21 linkage groups had two or more anchor loci predominantly found on HEE 7, including the majority of ribosomal protein genes *RpL5*, *RpS5*, *RpL10a*, *RpS8*, *RpP0*, which mapped along with two microsatellites *Hel-02* and *Hel-04*.

Sex chromosomes: As mentioned above, Z-tagged markers associate with two separate MI-identified linkage groups, Z and Z*. Each of these groups also contained an anchor locus associated with the sex chromosome. All but 2 of the loci in the larger group Z (7 censored-BI AFLPs, 1 MI AFLP, *Tpi*, and *He-CA-002*) were inherited from the *H. himera* paternal grandfather's Z chromosome (*i.e.*, these loci were in the same linkage phase). Furthermore, all but 1 of the small Z* loci were in the opposite linkage phase indicating they were inherited from the *H. erato etylus* paternal grandmother. These two linkage groups do not join until <LOD 4.0. This pattern may reflect a recombination hotspot on Z or reduced pairing of the two species' Z chromosomes during meiosis. However, in the absence of cytological evidence to the contrary, we chose to present the two clusters as a single linkage group, although there are insufficient data to orient the two clusters with respect to each other (Figure 2). Interestingly and somewhat surprisingly, despite scoring nearly 200 FI loci, we did not identify a single W-linked (female only) marker.

Recombination: In this study, we found an average of 3.1 crossover events per marker per chromosome averaged over all linkage groups (assuming half the double recombinants are valid crossover events). HEE d had the lowest estimate (1.7 per marker) and HEC Z had the highest estimate (4.8 crossover events per marker). When estimated across autosomes the average number of recombination events per cM was 0.59 (range 0.35–0.94). The two linkage groups associated with Z were the lowest (0.32 crossovers per cM) and the highest (1.38 crossovers per cM).

Mapping color pattern loci: The two color pattern loci, *Sd* and *D*, mapped to linkage groups HEE 6 and HEC 3, respectively. When scored as a typical BI locus the 95% confidence interval for *Sd* is 21.5 cM bracketed by markers LTAA169 and TCCT138 (Figure 3A). However, the MI c-spot allowed a tighter placement of this locus, decreasing the 95% confidence interval containing the *Sd* locus to an 8.8-cM region defined by three AFLP bands on linkage group HEE 6 where the maximum likelihood interval (~75% of the probability density) is a 6.3-cM window flanked by two MI markers, TCAC466 and ACCA167 (Figure 3A). Utilizing the metabulks to find additional loci linked to *Sd* produced two further loci: CCTAmbA ~5.6 cM above the maximum likelihood position and CCTTSd ~12.9 cM below the maximum likelihood position.

On the basis of initial mapping the *D* locus was similarly localized, mapping ~3 cM terminal to TCAC242 on HEC 3. To bracket *D* we searched for additional markers using metabulks organized around *D* described in MATERIALS AND METHODS (see Table 1 legend for details). These scans revealed two additional TCTADRY and CCAC491 loci linked to *D*. With the addition of these loci the 95% confidence limits showed this locus to be either 2–3 cM beyond the terminal marker or in the 9.4 cM region between marker CCAC491 and TCTADRY (Figure 3B). Unlike the two spot alleles of the *Sd* locus, the *D* locus did not show 1:1 phenotypic effects. However, by specifically following the *H. erato etylus D* allele [*D* (MI)] of the male parent, predicted by association with the chromosome print (see solid bars in Figure 3B and supplemental Appendix at http://www.genetics.org/supplemental/), we are able to double the number of informative offspring and show the maximum likelihood position of *D* is the 6.7-cM interval between CCAC491 and TCAC242 at the end of linkage group HEC 3 (~70% of the probability density, Figure 3B, black bars).

DISCUSSION

Heliconius butterflies are renowned for their diversity of brilliant mimetic wing color patterns, making them a model clade for studying adaptive radiation, mimicry, natural selection, and speciation (EMSLEY 1965; BENSON 1972; GILBERT 1972, 2003; TURNER 1984; MALLET *et al.* 1990, 1998; MALLET 1993; BROWER 1994, 1996; SRYGLEY 1999; JIGGINS *et al.* 2001; KAPAN 2001; BELTRÁN *et al.* 2002; NAISBIT *et al.* 2003; FLANAGAN *et al.* 2004; LANGHAM 2005). Uniquely, the radiation in Heliconius warning color patterns couples both divergent evolution within species and multiple independent cases of convergent evolution between distantly related species (TURNER 1983, 1984; BROWER 1996; MALLET *et al.* 1998; FLANAGAN *et al.* 2004). This pattern of divergent and convergent evolution is best exemplified in *H. erato* and *H. melpomene*, two distantly related species that share identical wing pattern phenotypes due to Müllerian mimicry where they co-occur, as well as displaying parallel geographic patterns of divergence across Central and South America (TURNER 1983). Warning color variation in both species is controlled by a handful of loci with major phenotypic effects (SHEPPARD *et al.* 1985), which raises questions about the exact nature of the loci involved and the extent that analogous color pattern changes in the two species are caused by changes in homologous loci. Are phenotypic changes caused by changes in regulatory regions, gene duplications, or possibly adaptive recombination to form linkage among previously unlinked pattern elements? Are the highly similar wing pattern elements derived from strictly homologous building blocks, or are different loci used to create nearly identical phenotypic patterns? Answers to these questions will elucidate fundamental processes of the evolution of adaptive phenotypes and will advance our understanding of how evolutionary

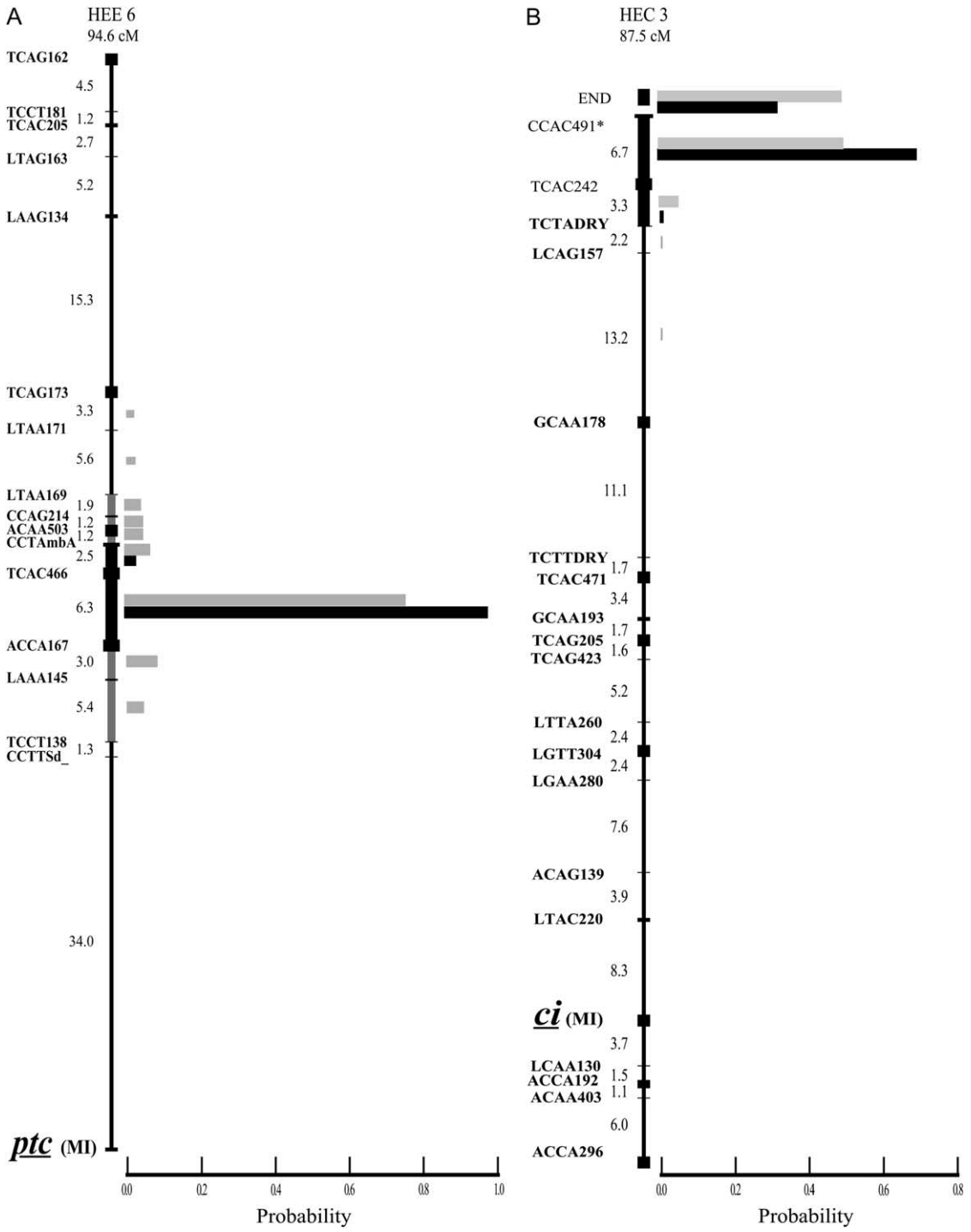

FIGURE 3.—Placement of color pattern loci *Sd* (A) and *D* (B). Horizontal bars represent the probability that the gene locus responsible for the phenotypic effects seen in the cross is located in the interval between the marker loci on a fixed map calculated from the antilog of the base ten log-likelihoods of linkage for each interval returned with the Mapmaker "try" command, normalized by the sum of these transformed values for all intervals including unlinked (VEILAND 1998). Absence of a bar indicates an effectively zero probability that the locus occurs in the interval. The broad map backbones indicate the ~95% confidence regions where color pattern loci occur (≤LOD 2.0 units from maximum likelihood position) as gray bars for BI scoring and as black bars for MI scoring. In A, the BI scoring of the codominant *Sd* phenotype is represented by gray bars, while the black bars represent the 1:1 MI scoring of the c-spot, likely an alternative allele of *Sd* (see RESULTS and DISCUSSION). In B, the *D* locus is shown with the BI scoring as gray bars and the 1:1 MI scores following the *H. erato etylus D* allele of the male parent as black bars (see MATERIALS AND METHODS). Note, in B the 95% confidence limits are the same for both BI and MI scorings.

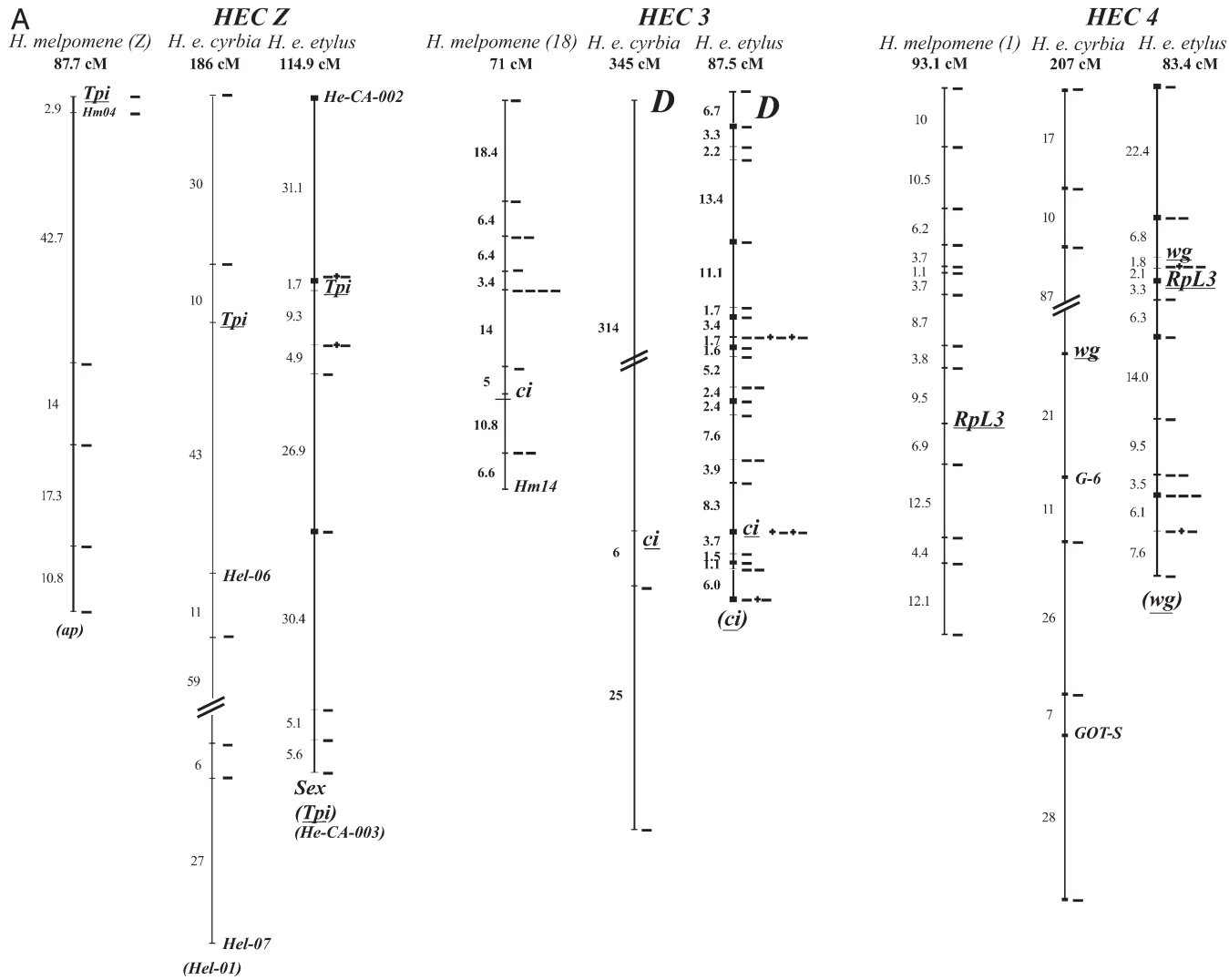

FIGURE 4.—Comparison of linkage results in the present study with linkage groups from corresponding studies: *H. melpomene* (left) (JIGGINS *et al.* 2005), *H. erato cyrbia* (center) (TOBLER *et al.* 2005), and *H. erato cyrbia* (right, this study) on the basis of shared codominant anchor loci. The density of AFLP markers is indicated by horizontal tick marks at each framework location. AFLP loci forming haplotypes are joined by + signs. (A) All linkage groups originally identified in TOBLER *et al.* (2005) and also identified in JIGGINS *et al.* (2005). (B) Linkage groups originally identified in TOBLER *et al.* (2005) not yet found in *H. melpomene*. (C) Linkage groups with tentative homology between present study and *H. melpomene* (JIGGINS *et al.* 2005). A–C are drawn to different scales.

change is constrained by preexisting genetic variation and/or developmental processes.

As our second step toward the genetic and developmental dissection of convergent and divergent evolution in Heliconius, we report the first high-resolution genetic map for *H. erato*. This new map is a considerable advance over our preliminary work on *H. erato* (TOBLER *et al.* 2005) and similar in density to the genetic linkage map recently published for *H. melpomene* (JIGGINS *et al.* 2005). It is based on segregation of markers in a much larger brood and contains over three times the number of loci. This combination reduces the average intermarker distance nearly fourfold to 5.1 cM and decreases the coefficient of variation of linkage group size by >200%. The new map provides a stable backbone for localizing the color pattern genes responsible for *H. erato*'s interracial diversification within the genome and relative to potential candidate loci (Figure 2). Furthermore, this map is an important reference for continued linkage analysis in Heliconius. In total, 13 shared SCNL (of 18 possible) and one microsatellite (Hm06) were mapped to eight linkage groups in both *H. erato* and *H. melpomene* (JIGGINS *et al.* 2005) allowing for the first direct comparisons of the genetic architecture underlying the replicate color pattern radiations (Figure 4).

Genetic basis of divergent evolution—mapping color pattern genes in *H. erato*: *H. erato* has the advantage that the various patterning loci can be studied by crossing different races to the same stock of its sister species *H. himera*. For example, in our *H. erato etylus* × *H. himera* broods, both *D* and *Sd* phenotypes are codominant and have complementary effects leading to expected single

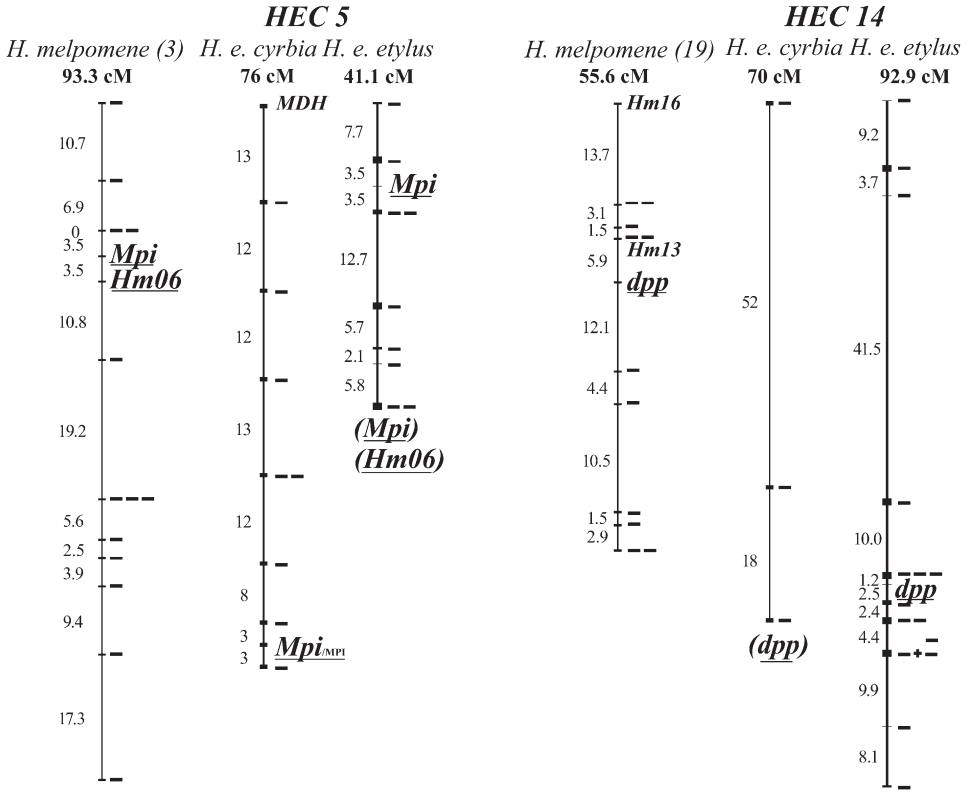

Figure 4.—*Continued.*

locus 1:2:1 and two locus 9:3:3:1 offspring ratios in F_2 style crosses (Figure 1). In addition, scoring of both loci is simplified because of the absence of epistasis when crossed with *H. himera*, which is normally seen in interracial crosses among many of the loci responsible for pattern variation in Heliconius (Mallet 1989; Jiggins and McMillan 1997; Gilbert 2003; Naisbit *et al.* 2003; Tobler *et al.* 2005).

Between Tobler *et al.* (2005) and the present study we have now mapped three color pattern loci in *H. erato* (*D*, *Sd*, and *Cr*). The *D* locus affects red and orange color pattern elements across the fore- and hindwing; in contrast, both the *Sd* and the *Cr* loci affect the pattern of melanization in the fore- and hindwing of *H. erato* and *H. himera* (Sheppard *et al.* 1985; Mallet 1989; Jiggins and McMillan 1997). All three loci are linked to codominant loci, which act as important anchors for integrating different mapping projects within species and for comparing the patterns of synteny between species (see below). For example, we can now demonstrate homology of hypothesized *D* locus phenotypic effects across *H. himera*, *H. erato cyrbia*, and *H. erato etylus* (as was hypothesized by Jiggins and McMillan 1997; Tobler *et al.* 2005). The *D* locus segregates in both our *H. himera* × *H. erato cyrbia* and *H. himera* × *H. erato etylus* crosses. In both crosses, the locus maps to the end of the same linkage group containing the SCNL *Cubitus interruptus* (*Ci*) (Tobler *et al.* 2005). Additional F2 crosses between *H. himera* and *H. erato cyrbia* (three crosses, 259 offspring) and *H. erato etylus* (five additional crosses, total of 598 offspring) performed in our lab show identical results with Mendelian segregation of *D* and no recombinants observed between *D* locus pattern elements arising from *H. himera* and *H. erato* (D. D. Kapan and W. O. McMillan, unpublished data).

AFLPs are a valuable tool for investigating unexplored genomes (Parsons and Shaw 2002) and serve several important functions in our ongoing mapping efforts in Heliconius. Foremost, they allow the tight localization of particular color pattern loci on a dense map. In this study, with only 20 primer combinations, we mapped over 350 segregating AFLP loci in our interspecific cross. This level of marker coverage allowed us to narrow the maximum likelihood interval containing the *Sd* locus to 6.3-cM region flanked by two AFLP bands on linkage group HEE 6. With the addition of several new primer combinations we were similarly able to flank the *D* locus in a 6.7-cM interval near the end of linkage group HEC 3. Given the estimated recombination length of 1430 Haldane cM and a physical size of ~395 Mb (Tobler *et al.* 2005) and assuming a one-to-one correspondence between physical and recombination size suggests an interval size of ~1.7 Mb (~2.4 Mb 95% CI) for the *Sd* and 1.9 Mb (~3.5 Mb 95% CI) for the *D* locus. Of course the relationship between physical and recombination size is likely to be complex (McVean *et al.* 2004); however, our estimates are conservative and there are several AFLP bands segregating in our screen of 88 offspring that were only one to two recombinants distant from the two major color pattern loci. This level

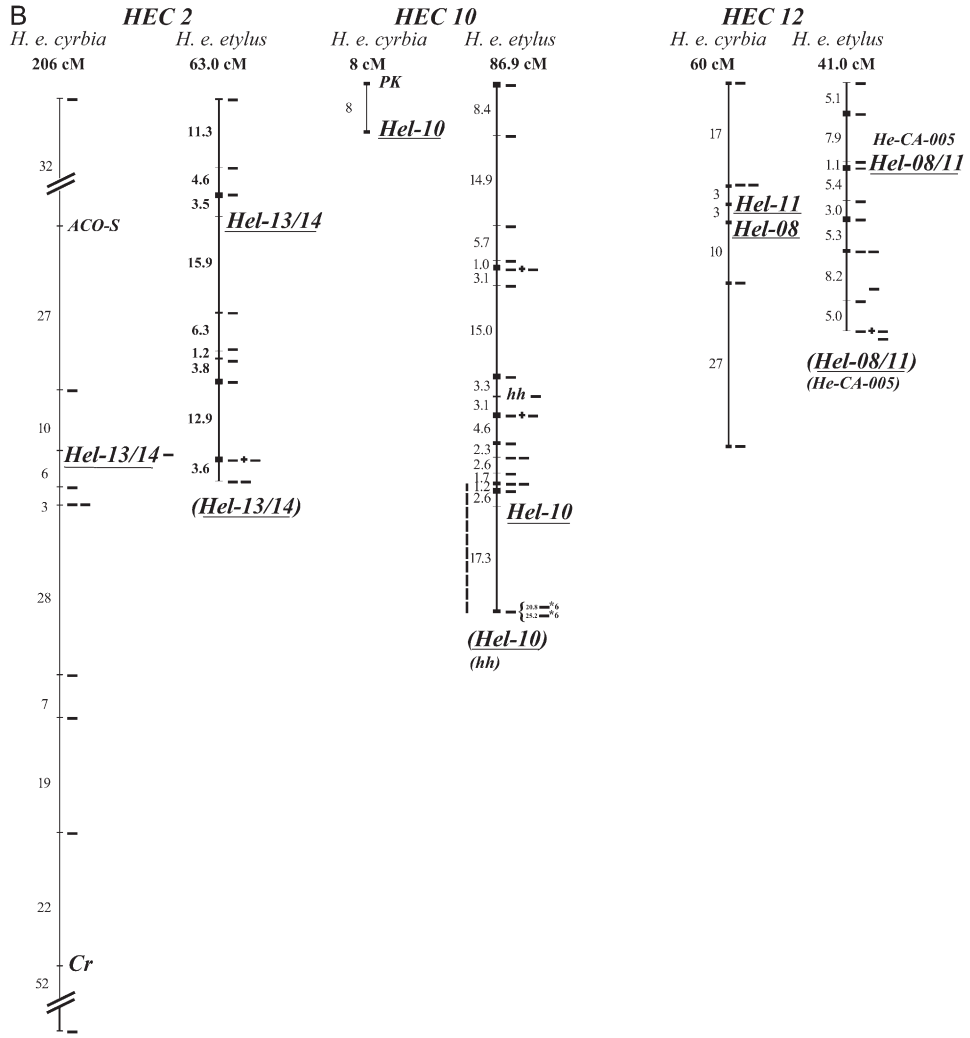

Figure 4.—*Continued.*

of recombination is within the estimated error that we encountered when mapping with dominant AFLP markers.

Second, AFLP loci identified in this and other genetic screens of Heliconius broods provide a ready supply of new loci tightly linked to color pattern loci and with further development can be an important source of codominant loci for ongoing high-resolution mapping studies. Using a combination of traditional mapping and color pattern metabulking we have found a number of AFLP fragments tightly linked to *Sd* and *D*. We have now isolated, cloned, and sequenced several of these linked AFLP including the terminal marker on HEC 3 that is tightly linked to *D* and have scored this marker in another large cross between *H. himera* and the very distinctive east Ecuadorian race *H. erato notabalis* (K. Maldonado, H. A. Merchan Gonzalez, D. D. Kapan and W. O. McMillan, unpublished results). In *H. notabalis* the *D* allele places a small patch of red scales in the distal portion of the area of the wing between veins Cu_1a and Cu_1b in a background of otherwise white scales. Between these two broods this marker shows a total of four potential recombinants across >200 offspring, suggesting that it is ≤2 cM from *D* (K. Maldonado, H. A. Merchan Gonzalez, D. D. Kapan and W. O. McMillan, unpublished results).

AFLP markers will also be important for placing color pattern loci that do not clearly segregate together on a common reference map of the *H. erato* color pattern radiation. For example, the *Cr* locus does not segregate in *H. himera* × *H. erato etylus* crosses, but is on group HEC 2 on the basis of linkage to the microsatellite *Hel 13/14* (Tobler *et al.* 2005) (Figure 4B). However, the inflated size of HEC 2 estimated by Tobler *et al.* (2005) makes it impossible to more tightly localize *Cr* on the current map due to the extreme distances between *Cr* and the two segregating anchor loci (*Hel 13/14*, 87 cM, and allozyme ACO-S, 124 cM), both greater than the entire length of HEC 2 in the present study (63.0 cM, Figure 4B). As an alternative, we are currently using the color pattern metabulking strategy to develop AFLP loci around *Cr* that will work across different mapping experiments by targeting flanking loci and converting these into anchor loci (see above). Given the high level of epistasis among major color pattern loci in Heliconius, the development of these genomic anchors will

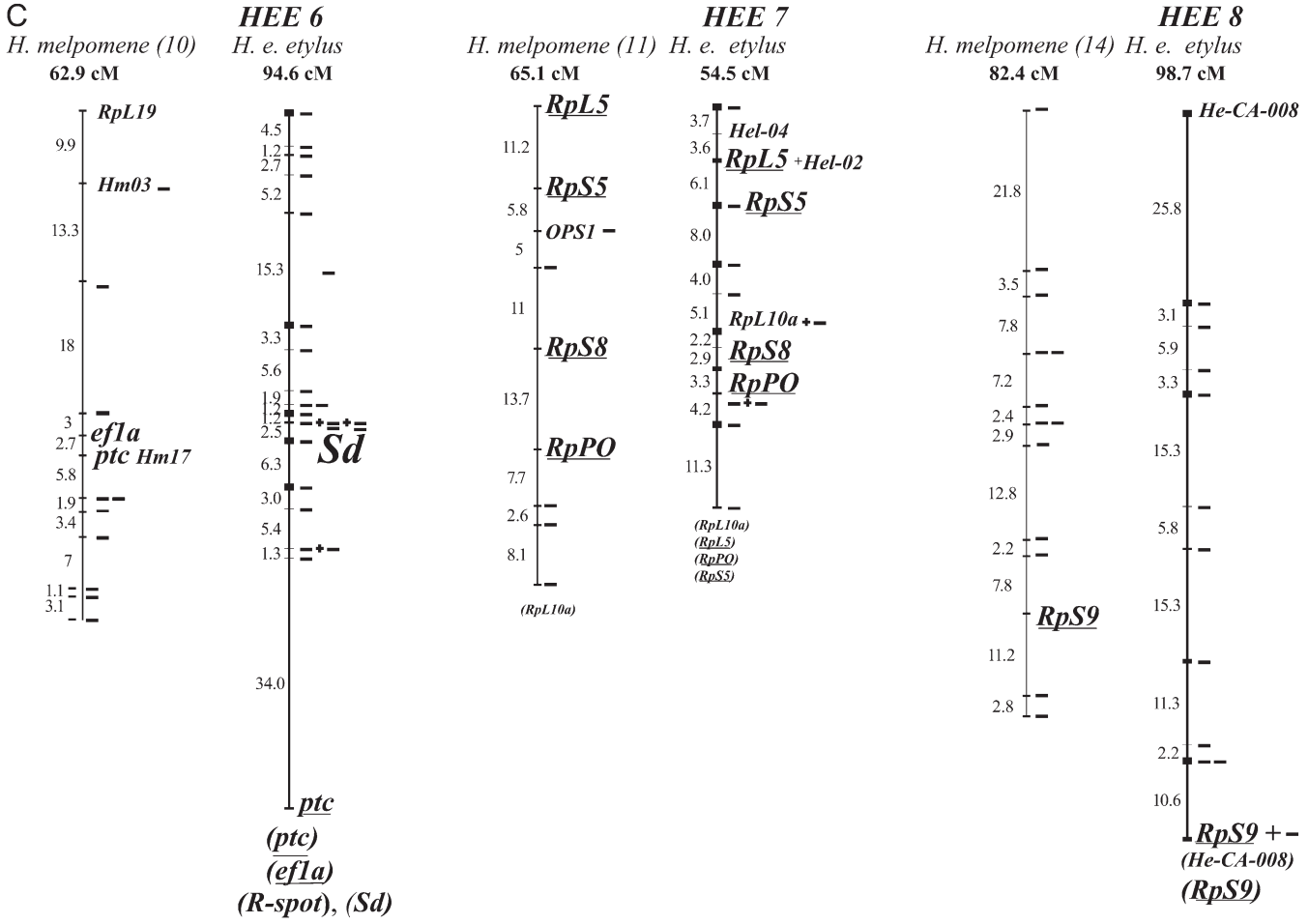

Figure 4.—*Continued.*

further refine our understanding of the broad phenotypic effects of color pattern loci in Heliconius.

Candidate loci: Our new high-resolution Heliconius linkage map allows us to test for the association between candidate loci, chosen on the basis of knowledge of gene action in other organisms, and color pattern genes. This candidate gene approach has been very successful in other organisms. For example, genes known to be involved in wing development in Drosophila were found to have novel but related roles in pattern specification in butterflies (Carroll *et al.* 1994; Brakefield *et al.* 1996; Koch *et al.* 1998, 2000; Keys *et al.* 1999; Brunetti *et al.* 2001; Reed and Gilbert 2004; Reed and Serfas 2004) and variation at one of these loci, *distal-less*, is speculated to cause variation in eyespot size in selected lines of *B. anayana* (Beldade *et al.* 2002). In Heliconius, the candidate gene approach has allowed us to eliminate several potential candidates for color pattern loci. Between this study and Tobler *et al.* (2005) we have excluded genes that play a role in either development or pigment synthesis as candidates for *D*, *Cr*, and *Sd*. The extracellular signaling ligand genes *wingless*, *decapentaplegic*, and *hedgehog*, the hedgehog receptor gene *patched*, the eyespot-associated transcription factor gene *cubitus interruptus*, and the ommochrome pigment synthesis enzyme gene *cinnabar* do not show strong linkage with any of three mapped color pattern genes (Figure 4). However, these loci may be linked to other color pattern loci within *H. erato* that have not yet been mapped.

The comparative architecture of mimicry: The strong resemblance between *H. erato* and *H. melpomene* wing patterns has led researchers to speculate that homologous loci underlie the parallel radiations (Turner 1984; Nijhout 1991). This theory suggests that developmental constraints might have played a significant role in the evolution of convergent wing patterns (see Naisbit *et al.* 2003) and predicts that loci that have similar phenotypic effects in the two comimics should reside on the same chromosome and show similar patterns of synteny with nearby markers.

Using mapping data to detect genetic homology requires that genomic rearrangements have been minimal and that both gross- and fine-scale patterns of synteny are likely conserved between the two comimics. Although we have jointly mapped only a small number

of single copy nuclear genes in the two comimics thus far, these shared markers indicate that gene order is highly conserved. Indeed, there are no conflicting linkage relationships between *H. erato* and *H. melpomene*. The strongest support of the general conservation for linkage relationship within Heliconius comes from a cluster of ribosomal proteins (*RpL5*, *RpS5*, *RpL10a*, *RpS8*, and *RpPO*), all of which map to the same linkage group (HEE 7 and HMEL 11) and show conserved gene order (Figure 4). The conservation of linkage and the observation that both species of Heliconius have the same number of chromosomes is consistent with the hypothesis that there have not been many chromosome fusions or breakages since the two lineages diverged. On the basis of one or two shared codominant anchor loci per linkage group (Jiggins *et al.* 2005), we identified tentative homology between seven autosomal linkage groups as well as the Z chromosome between the two comimics (Figure 4). Although there was no correlation between the size of putatively homologous linkage groups ($r = -0.097$, $t_6 = -0.24$, $P > 0.59$), the overall spanning map size of the species was similar, 1430 Haldane cM in *H. erato vs.* 1616 cM in *H. melpomene* (Jiggins *et al.* 2005). This similarity is out of accord with the recent estimates of genome size, which suggest that *H. erato*'s genome is ~136% greater than that of *H. melpomene* (Jiggins *et al.* 2005). The slightly larger recombination length coupled with a smaller genome size of *H. melpomene* suggests that *H. melpomene* has a higher crossing over frequency than *H. erato*. This is intriguing in light of evidence that *H. erato* is almost always more abundant and may commonly act as the Müllerian model in this pair (Kapan 2001; Mallet 2001; Flanagan *et al.* 2004). If true, under these conditions *H. melpomene* may benefit from genomic flexibility provided by an increased crossing-over rate to track *H. erato* (see below).

To date, only one major color pattern locus, *Yb*, has been mapped in *H. melpomene* (Jiggins *et al.* 2005). The *Yb* locus controls the yellow elements on the dorsal and ventral hindwing surfaces in *H. melpomene* (Sheppard *et al.* 1985; Mallet 1989; Jiggins *et al.* 2005) and maps to *H. melpomene* group HMEL 15 along with two microsatellite loci, *Hm01* and *Hm08*. *Yb* is extremely tightly linked to *Sb*, which controls the white fringe on the hindwing of *H. m. cythera*, and to *N*, which controls the presence of melanin in the forewing some of Amazonian races (see Sheppard *et al.* 1985; Mallet 1989; Naisbit *et al.* 2003; Jiggins *et al.* 2005). *Yb/Sb/N* complex produces nearly identical phenotypes to the *Cr* locus in *H. erato*, which maps to HEC 2 based on the presence of the microsatellite *Hel-13/14* (Tobler *et al.* 2005) (Figure 2). Unfortunately, there are no cosegregating color pattern loci in common between the *H. erato* and *H. melpomene* maps for these linkage groups, but the color pattern homology hypothesis predicts that *Cr* and *Yb/Sb/N* will map to the homologous linkage group and will show similar linkage relationships to other loci in this group. An identical argument holds for the *D* locus in *H. melpomene* and the *D* locus in *H. erato*. Alleles at these loci have similar (but not identical) phenotypic effects in the two comimics and have been assumed to be homologous. In *H. erato* the *D* locus is loosely linked to *Ci*, suggesting that the *D* locus in *H. melpomene* should map to linkage group HMEL 18 in Jiggins *et al.* (2005), a prediction recently borne out by additional mapping work in *H. melpomene* (C. Jiggins, personal communication). There are several potential *H. melpomene* homologs to *H. erato*'s *Sd* locus as a number of loci affect melanin patterns (and therefore the shape, size, and position of yellow pattern elements) on the forewing of both species (Sheppard *et al.* 1985; Gilbert 2003); therefore, further mapping will be necessary to ascertain color pattern homologs for *Sd*.

Codominant anchor loci and continued linkage mapping in Heliconius: Strong arguments for or against color pattern homology will require comparing both broad- and fine-scale synteny. This will be especially important as many of the genes described in Heliconius have major phenotypic effects and some appear to be composed of complexes of tightly linked loci or supergenes (Sheppard *et al.* 1985; Mallet 1989; Nijhout 1991; Jiggins and McMillan 1997; Joron *et al.* 2001; Naisbit *et al.* 2003). One explanation for this pattern is that mimicry-related selection has favored stronger linkage between genes that work together to form specific adaptive color patterns. Adaptive evolution in linkage seems unlikely in Heliconius (see Naisbit *et al.* 2003 for discussion), but could be more important than previously envisioned if Müllerian mimicry evolution typically proceeds in a one-sided fashion where a rare species (in this case, *H. melpomene*) evolves similarity to (or adverges on) the pattern of a more common species (Mallet 2001; Kapan 2001, Flanagan *et al.* 2004). True integration of these maps necessitates the development of more anchor loci for defining the broad-scale patterns of synteny between the two comimics. Of the two codominant marker systems used in our mapping work, SCNL have proved to be much better anchors for comparative genomics in Heliconius. Only 2 (*Hel 05, Hm06*) of the >40 microsatellites developed for Heliconius could be mapped in the two species (Jiggins *et al.* 2005, Tobler *et al.* 2005). In contrast, over half of the 21 SCNL developed from candidate and housekeeping genes have been mapped or placed in linkage groups in both species (Table 4, Figure 4) (Jiggins *et al.* 2005; Tobler *et al.* 2005). Generating new gene-based markers in Heliconius is now extremely efficient using a growing EST database (http://heliconius.cap.edu.ac.uk/butterfly/db/, see Papanicolaou *et al.* 2005). Furthermore, because there is no crossing over during oogenesis in Lepidoptera (Suomalainen *et al.*, 1973) only a small number of individuals need to be typed to assign particular markers

to particular linkage groups. However, a large number of SCNL in both species will undoubtedly need to be typed to characterize the fine-scale patterns of synteny. In this respect, targeted AFLP loci can provide critical genomic anchors around color pattern loci. To date, primers designed around AFLP loci in one species have not worked in the other species (W. O. McMillan and C. D. Jiggins, unpublished data). Yet targeted AFLP loci are good probes for BAC libraries, which are available for both species, and gene-based markers tightly linked to color pattern genes are currently being developed from initial BAC sequences.

Conclusions and future directions: Developing linkage maps for Heliconius is critical if we are to build upon the long history of ecological and evolutionary work in this group to address questions concerning the interplay between selection and morphological diversification. The localization of two color pattern genes to narrow regions of two linkage groups follows a similar success for a single color pattern locus in *H. erato*'s distantly related comimic, *H. melpomene* (Jiggins *et al.* 2005). Both projects utilized a three-step mapping strategy that takes advantage of the diversity of segregation markers in natural populations (Jiggins *et al.* 2005; see supplemental Figure S1 at http://www.genetics.org/supplemental/). This technique is applicable to any outbred species with sex-restricted recombination, such as nearly all Lepidoptera. It relies on FI alleles segregating in an F2-style cross to generate a chromosomal contig or print (Yasukochi 1998) that is utilized to unambiguously identify linkage groups from markers recombining in the male parent. These Heliconius mapping projects serve as a foundation for the comparative study of the evolutionary genetic basis of mimicry, represent an important step toward obtaining targeted sequence data from genomic regions linked to genes underlying color pattern evolution, and promise to accelerate the identification and molecular characterization of the color pattern loci themselves. Ultimately, this work will help promote a wider understanding of how convergent morphologies arise in nature.

We thank Jim Mallet for his keen insights into color pattern genetics in Heliconius and comments on early versions of this manuscript and Chris Jiggins for assistance with Joinmap and early discussion of the three-step method prior to publication. We also thank the Ministerio del Ambiente in Ecuador for permission to collect butterflies and Germania Estévez for help and guidance during collecting trips. We give a special thanks to Ana Maria Quiles and many volunteers of the butterfly rearing crew for help rearing larvae and maintaining the Heliconius insectaries at the University of Puerto Rico. We thank also Wyndham Kapan for fully updating the program Genographer in JAVA (version 2.1 beta available at http://zephyr.hpcf.upr.edu/~mcmi-lab/). Finally, we thank Shannon N. Bennett and Valerie McMillan for critical review of the manuscript and Daniel Lindstrom for his support and editing. Undergraduate students participating in this project were supported in part by University of Puerto Rico's Research Initiative for Scientific Enhancement, Puerto Rico's Alliance for Minority Participation, and the University of Puerto Rico Rio Piedras' Center for Applied Tropical Ecology and Conservation. Puerto Rico Experimental Program to Stimulate Competitive Research program and Biomedical Research Infrastructure Network in Puerto Rico and the National Institutes of the Health Support of Continuous Research Excellence Program provided funding for the Sequencing and Genotyping Center at University of Puerto Rico Rio Piedras. Funding for this study was provided by National Science Foundation grants to W.O.M.

LITERATURE CITED

Albertson, R. C., J. T. Streelman and T. D. Kocher, 2003 Genetic basis of adaptive shape differences in the cichlid head. J. Hered. **94:** 291–301.

Beebe, W., 1955 Polymorphism in reared broods of *Heliconius* butterflies from Surinam and Trinidad. Zoologica **40:** 139–143.

Beldade, P., P. M. Brakefield and A. D. Long, 2002 Contribution of *Distal-less* to quantitative variation in butterfly eyespots. Nature **415:** 315–318.

Beltrán, M., C. D. Jiggins, V. Bull, M. Linares, W. O. McMillan *et al.*, 2002 Phylogenetic discordance at the species boundary: comparative gene genealogies among *Heliconius* butterflies. Mol. Biol. Evol. **19:** 2176–2190.

Benham, J., J.-U. Jeung, M. Jasieniu, V. Kanazin and T. Blake, 1999 Genographer: a graphical tool for automated AFLP and microsatellite analysis. Article 3, Journal of Agricultural Genomics. Published with permission from CAB International. Full text available from http://www.cabi-publishing.org/JAG

Benson, W. W., 1972 Natural selection for Müllerian mimicry in *Heliconius erato* in Costa Rica. Science **176:** 936–939.

Bradshaw, H. D., Jr., K. G. Otto, B. E. Frewen, J. K. McKay and D. W. Schemske, 1998 Quantitative trait loci affecting differences in floral morphology between two species of monkeyflower (Mimulus). Genetics **149:** 367–382.

Brakefield, P. M., J. Gates, D. Keys, F. Kesbeke, P. J. Wijngaarden *et al.*, 1996 Development, plasticity, and evolution of butterfly eyespot patterns. Nature **384:** 236–242.

Brower, A. V. Z., 1994 Rapid morphological radiation and convergence among races of the butterfly *Heliconius erato* inferred from patterns of mitochondrial DNA evolution. Proc. Natl. Acad. Sci. USA **91:** 6491–6495.

Brower, A. V. Z., 1996 Parallel race formation and the evolution of mimicry in *Heliconius* butterflies: a phylogenetic hypothesis from mitochondrial DNA sequences. Evolution **50:** 195–221.

Brown, K. S., P. M. Sheppard and J. R. G. Turner, 1974 Quaternary refugia in tropical America: evidence from race formation in *Heliconius* butterflies. Proc. R. Soc. Lond. Ser. B **187:** 369–378.

Brown, K. S., T. C. Emmel, P. J. Eliazar and E. Soumalainen, 1992 Evolutionary patterns in chromosome numbers of Neotropical Lepidoptera. I. Chromosomes of the Heliconiini (family Nymphalidae: subfamily Nymphalinae). Hereditas **117:** 109–125.

Brunetti, C. R., J. E. Selegue, A. Monteiro, V. French, P. M. Brakefield *et al.*, 2001 The generation and diversification of butterfly eyespot color patterns. Curr. Biol. **11:** 1578–1585.

Carroll, S. B., J. Gates, D. N. Keys, S. W. Paddock, G. E. F. Panganiban *et al.*, 1994 Pattern formation and eyespot determination in butterfly wings. Science **265:** 109–114.

Chai, P., 1986 Field observations and feeding experiments on the responses of rufous-tailed jacamars (*Galbula ruficauda*) to free-flying butterflies in a tropical rainforest. Biol. J. Linn. Soc. **29:** 166–189.

Colosimo, P. F., K. E. Hosemann, S. Balabhadra, G. Villarreal, Jr., M. Dickson *et al.*, 2005 Widespread parallel evolution in sticklebacks by repeated fixation of ectodysplasin alleles. Science **307:** 1928–1933.

Emsley, M. G., 1963 A morphological study of imagine Heliconiinae (Lep.: Nymphalidae) with a consideration of the evolutionary relationships within the group. Zoologica **48:** 85–130.

Emsley, M. G., 1965 Speciation in *Heliconius* (Lep. Nymphalidae): morphology and geographic distribution. Zoologica **50:** 191–254.

Flanagan, N. S., M. Blum, A Davison, M Alamo, R Albarran *et al.*, 2002 Characterization of microsatellite loci in neotropical *Heliconius* butterflies. Mol. Ecol. Notes **2:** 398–401.

Flanagan, N., A. Tobler, D. Kapan, A. Davison, O. Pybus *et al.*, 2004 Historical demography of Müllerian mimicry in the

Neo-tropical *Heliconius* butterflies. Proc. Natl. Acad. Sci. USA **101:** 9704–9709.

Gilbert, L. E., 1972 Pollen feeding and reproductive biology of *Heliconius* butterflies. Proc. Natl. Acad. Sci. USA **69:** 1403–1407.

Gilbert, L. E., 2003 Adaptive novelty through introgression in *Heliconius* wing patterns: evidence for shared genetic "toolbox" from synthetic hybrid zones and a theory of diversification, pp. 281–318 in *Ecology and Evolution Taking Flight: Butterflies as Model Systems*, edited by C. L. Boggs, W. B. Watt and P. R. Ehrlich. University of Chicago Press, Chicago.

Gilbert, L. E., H. S. Forrest, T. D. Schultz and D. J. Harvey, 1988 Correlations of ultrastructure and pigmentation suggest how genes control development of wing scales of *Heliconius* butterflies. J. Res. Lepid. **26:** 141–160.

Hoekstra, H. E., K. E. Drumm and M. W. Nachman, 2004 Ecological genetics of adaptive color polymorphism in pocket mice: geographic variation in selected and neutral genes. Evolution **58:** 1329–1341.

Jiggins, C. D., and W. O. McMillan, 1997 The genetic basis of an adaptive radiation: warning colour in two *Heliconius* species. Proc. R. Soc. Lond. Ser. B **246:** 1167–1175.

Jiggins, C. D., R. E. Naisbit, R. L. Coe and J. Mallet, 2001 Reproductive isolation caused by colour pattern mimicry. Nature **411:** 302–305.

Jiggins, C. D., J. Mavarez, M. Beltrán, W. O. McMillan, S. Johnston *et al.*, 2005 A genetic linkage map of the mimetic butterfly *Heliconius melpomene*. Genetics **171:** 557–570.

Joron, M., I. R. Wynne, G. Lamas and J. Mallet, 2001 Variable selection and the coexistence of multiple mimetic forms of the butterfly *Heliconius numata*. Evol. Ecol. **13:** 721–754.

Kapan, D. D., 2001 Three-butterfly system provides a field test of Müllerian mimicry. Nature **409:** 338–340.

Keys, D. N., D. L. Lewis, J. E. Selegue, B. J. Pearson, L. V. Goodrich *et al.*, 1999 Recruitment of a hedgehog regulatory circuit in butterfly eyespot evolution. Science **283:** 532–534.

Koch, P. B., D. N. Keys, T. Rocheleau, K. Aronstein, M. Blackburn *et al.*, 1998 Regulation of dopa decarboxylase expression during colour pattern formation in wild-type and melanic tiger swallowtail butterflies. Development **125:** 2303–2313.

Koch, P. B., U. Lorenz, P. M. Brakefield and R. H. Ffrench-Constant, 2000 Butterfly wing pattern mutants: developmental heterochrony and co-ordinately regulated phenotypes. Dev. Genes Evol. **210:** 536–544.

Langham, G. M., 2005 Specialized avian predators repeatedly attack novel color morphs of *Heliconius* butterflies. Evolution **58:** 2783–2787.

Lincoln, S. E., and E. S. Lander, 1992 Systematic detection of errors in genetic linkage data. Genomics. **14:** 604–610.

Lincoln, S. E., M. J. Daly and E. S. Lander, 1987 MAPMAKER 3.0. Whitehead Institute for Biomedical Research/MIT Center for Genome Research, Boston.

Mallet, J., 1989 The genetics of warning colour in Peruvian hybrid zones of *Heliconius erato* and *H. melpomene*. Proc. R. Soc. Lond. Ser. B **236:** 163–185.

Mallet, J., 1993 Speciation, raciation, and color pattern evolution in *Heliconius* butterflies: evidence from hybrid zones, pp. 226–260 in *Hybrid Zones and the Evolutionary Process*, edited by R. G. Harrison. Oxford University Press, New York.

Mallet, J., 2001 Causes and consequences of a lack of coevolution in Müllerian mimicry. Evol. Ecol. **13:** 777–806.

Mallet, J., N. H. Barton, G. Lamas, J. Santisteban, M. Muedas *et al.*, 1990 Estimates of selection and gene flow from measures of cline width and linkage disequlibrium in Heliconius hybrid zones. Genetics **124:** 921–936.

Mallet, J., W. O. McMillan and C. D. Jiggins, 1998 Mate choice between a pair of *Heliconius* species in the wild. Evolution **52:** 503–510.

McMillan, W. O., C. D. Jiggins and J. Mallet, 1997 What initiates speciation in passion-vine butterflies? Proc. Natl. Acad. Sci. USA **94:** 8628–8633.

McVean, G. A. T., S. R. Myers, S. Hunt, P. Deloukas, D. R. Bentley *et al.*, 2004 The fine-scale structure of recombination rate variation in the human genome. Science **304:** 581–584.

Michelmore, R. W., I. Paran and R.V. Kesseli, 1991 Identification of markers linked to disease-resistance genes by bulked segregant analysis: a rapid method to detect markers in specific genomic regions by using segregating populations. Proc. Natl. Acad. Sci. USA **88:** 9828–9832.

Müller, F., 1879 *Ituna* and *Thyridia*; a remarkable case of mimicry in butterflies. Trans. Entomol. Soc. **1879:** xx–xxix.

Nachman, M. W., H. E. Hoekstra and S. L. D'Agostino, 2004 The genetic basis of adaptive melanism in pocket mice. Proc. Natl. Acad. Sci. USA **100:** 5268–5273.

Naisbit, R. E., C. D. Jiggins and J. Mallet, 2003 Mimicry: developmental genes that contribute to speciation. Evol. Dev. **5:** 269–280.

Nijhout, H. F., 1991 *The Development and Evolution of Butterfly Wing Patterns*. Smithsonian Institution Press, Washington, DC.

Nijhout, H. F., G. A. Wray and L. E. Gilbert, 1990 An analysis of the phenotypic effects of certain colour pattern genes in *Heliconius* (Lepidoptera: Nymphalidae). Biol. J. Linn. Soc. **40:** 357–372.

Papanicolaou, A., M. Joron, W. O. McMillan, M. L. Blaxter and C. D. Jiggins, 2005 Genomic tools and cDNA derived markers for butterflies. Mol. Ecol. **14:** 2883–2897.

Parsons, Y. M., and K. L. Shaw, 2002 Mapping unexplored genomes: a genetic linkage map of the Hawaiian cricket Laupala. Genetics **162:** 1275–1282.

Peichel, C. L., K. S. Nereng, K. A. Ohgi, B. L. E. Cole, P. F. Colosimo *et al.*, 2001 The genetic architecture of divergence between threespine stickleback species. Nature **414:** 901.

Reed, R. D., and L. E. Gilbert, 2004 Wing venation and *Distal-less* expression in *Heliconius* butterfly wing pattern development. Dev. Genes Evol. **214:** 628–634.

Reed, R. D., and M. S. Serfas, 2004 Butterfly wing pattern evolution is associated with changes in a *notch/distal-less* temporal pattern formation process. Curr. Biol. **14:** 1159–1166.

Sheppard, P. M., J. R. G. Turner, K. S. Brown, W. W. Benson and M. C. Singer, 1985 Genetics and the evolution of Müllerian mimicry in *Heliconius* butterflies. Philos. Trans. R. Soc. Lond. Ser. B **308:** 433–613.

Shi, J., D. G. Heckel and M. R. Goldsmith, 1995 A genetic linkage map for the domesticated silkworm, Bombyx mori, based on restriction fragment length polymorphisms. Genet. Res. **66:** 109–126.

Srygley, R. B., 1999 Locomotor mimicry in *Heliconius* butterflies: contrast analyses of flight morphology and kinematics. Philos. Trans. R. Soc. Lond. B **354:** 203–214.

Suomalainen, E., L. M. Cook and J. R. G. Turner, 1971 Chromosome numbers of heliconinne butterflies from Trinidad, West Indies (Lepidoptera, Nymphalidae). Zoologica **56:** 121–124.

Suomalainen, E., L. M. Cook and J. R. G. Turner, 1973 Achiasmatic oogenesis in the heliconiine butterflies. Hereditas **74:** 302–304.

Tobler, A., D. Kapan, N. Flanagan, C. Gonzalez, E. Peterson *et al.*, 2005 First generation linkage map of H. erato. Heredity **94:** 408–417.

Turner, J. R. G., 1974 Mimetic butterflies and punctuated equilibria: some old light on a new paradigm. Biol. J. Linn. Soc. **20:** 277–300.

Turner, J. R. G., 1983 Mimetic butterflies and punctuated equilibria: some old light on a new paradigm. Biol. J. Linn. Soc. **20:** 277–300.

Turner, J. R. G., 1984 Mimicry: the palatability spectrum and its consequences, pp. 141–161 in *The Biology of Butterflies*, edited by R. I. Vane-Wright and P. R. Ackery. Academic Press, London.

Turner, J. R. G., and J. Smiley, 1975 Absence of crossing-over in female butterflies (*Heliconius*). Heredity **34:** 265–269.

Turner, J. G. R., and J. L. B. Mallet, 1997 Did forest islands drive the diversity of warningly coloured butterflies? Biotic drift and the shifting balance. Philos. Trans. R. Soc. Lond. B **351:** 835–845.

Van Ooijen, J. W., and R. E. Voorrips, 2001 JoinMap 3.0: software for the calculation of genetic linkage maps. Plant Research International, Wageningen, The Netherlands.

Veiland, V., 1998 Bayesian linkage analysis, or: how I learned to stop worrying and love the posterior probability of linkage. Am. J. Hum. Genet.. **63:** 947–954.

Vos, P., R. Hogers, M. Bleeker, M. Reijans, T. van de Lee *et al.*, 1995 AFLP: a new technique for DNA fingerprinting. Nucleic Acids Res. **23:** 4407–4414.

Yasukochi, Y., 1998 A dense genetic map of the silkworm, *Bombyx mori*, covering all chromosomes based on 1018 molecular markers. Genetics **150:** 1513–1525.

Communicating editor: D. A. Long